Volume V
Appendix G.8

Using the Data and Observations from Flight STS-107... Exec Summary

This Appendix contains the report Using the Data and Observations From Flight STS-107 to Explain the Fatal Reentry of the Columbia Orbiter OV-102, Bertin, John J., Smiley, James W. This report develops possible scenarios that were considered by the Columbia Accident Investigation Board.

THIS PAGE INTENTIONALLY LEFT BLANK

USING THE DATA AND OBSERVATIONS FROM FLIGHT STS-107 TO EXPLAIN THE FATAL REENTRY OF THE COLUMBIA ORBITER OV-102

By
DR. JOHN J. BERTIN
DR. JAMES W. SMILEY
CONSULTANTS, CAIB SUPPORT GROUP

EXECUTIVE SUMMARY

In our role as Aerothermodynamic Consultants to the Columbia Accident Investigation Board (CAIB), we are documenting our interpretation of the key events, which led to the demise of OV-102 during Flight STS-107. In order to develop an understanding of aerothermodynamic environment and of the sequence of critical events that led to the demise of the Orbiter, meetings were held with NASA personnel and their contractors and with other consultants to Group 3 (Engineering and Technical Analysis) of the Columbia Accident Investigation Board (CAIB). During these meetings, we obtained film clips, timelines, basic data, interpretations of the data, and figures from power-point presentations. In these meetings, we exchanged ideas on what we thought were key events, about what was possible, what was likely, what was not possible, and what was not likely.

The authors would like to acknowledge the inputs (verbal and written) that we received from Rick Barton, Charles Campbell, Joe Caram, Ray Gomez, Dave Kanipe, Steve Labbe, Gerald J. Lebeau, Chris Madden, Fred Martin, Scott Murray, et al. [all of the Johnson Space Center (NASA)]; Stan Bouslog of Lockheed-Martin; and Jim Arnold, Howard Goldstein, Pat Goodman, Robert Hammond, Jim Mosquera, and Donald J. Rigali from the CAIB Technical Support Team. The authors have benefited from discussions with and from presentations made by the Group 3 members of the CAIB, Dr. James Hallock, G. Scott Hubbard, Dr. Doug Osherhoff, Roger Tetrault, and Dr. Sheila Widnall. The following text offers our interpretation of the significance of and the relationship between data and observations that are currently “known” about the fatal aerothermodynamic environment of flight STS-107 for the Columbia Orbiter, OV-102.

It is the intent of the authors to document a summary of key data and provide a realistic scenario that would explain the aerothermodynamic environment during the demise of Columbia OV-102. In this effort, we have attempted to match what we consider to be twelve critical events or observations that were determined from “data” gathered from the persons mentioned in the previous paragraph. The word “data” has been placed in quotes, since some “data” represent flight measurements whose time and magnitude are well known, other “data” represent debris whose origin and timing is somewhat subjective, and still other “data” are from computations and wind-tunnel tests and, thus, are dependent on the simulation models (numerical or experimental) used. Therefore, some of the observations based on our interpretation of the “data” may differ from the demise scenarios proposed by others using the same “data”. For instance, some of the information gleaned from the recovered debris may be in error, because the debris was misidentified or because the damage to the recovered debris may have occurred at a different time during the reentry. Furthermore, new information (in the form of additional recovered debris, analysis, etc.) may become available at some point in the future. For instance, data from the MADS recorder that was recovered after initial

investigations provided information over a longer time frame and from additional sensors. To allow for such uncertainties in the existing "data" and for the probability of new, additional data providing an improved understanding of the aerothermodynamic environment, most of the observations that the authors deem to be "critical" represent several pieces of information rather than a single datum point.

Furthermore, by matching the information from twelve "critical data/events", it is hoped that a reasonably accurate and coherent description of the evolving damage will be presented in this report. We will describe how the following sequence of events can be used to define a demise scenario, which is judged to be consistent with all of the "data".

1. The observation that foam particles from the external tanks impinged on the wing leading edge during the launch.

2. Radar signatures from the second day of the mission that showed a piece of debris drifting away from the Orbiter.

3. The strain-gage reading (beginning at EI + 270) and the temperature rise at two thermocouples located in the vicinity of RCC Panel 9 (beginning at EI + 290), as indicated by MADS data.

4. The perturbations to the heating and to the surface pressures due to the interaction between the bow shock wave and the wing-leading-edge shock wave are most severe in the region of RCC Panels 8 and 9.

5. Start of off nominal temperature histories at four sensors on left OMS Pod (beginning with lower than expected temperatures at EI + 340, followed by higher than expected temperatures at EI + 460).

6. The anomalous temperature increases that occurred at various locations in the main left-landing-gear wheel well (beginning at EI + 488).

7. The increase in temperatures at points located on the vertical side of the fuselage, as indicated both in thermocouples on the Orbiter itself and in the temperature sensitive coatings on the wind-tunnel models tested at the Langley Research Center (beginning at EI + 493).

8. Loss of all measurements from the wire bundle running along the backside of the wing spar (beginning at EI + 487) followed by the loss of measurements from the wire bundle running along the left main-landing gear wheel well, which included elevon measurements (beginning at EI + 527)

9. The observations regarding the damage to the wing leading edge, as determined from the recovered debris.

10. The modifications to the shock/shock interaction flow field that was described in "critical data/event" #4, as developed based on the developing damage scenario and correlated against the Kirtland photograph, i. e., observations by personnel from the Starfire Optical Range (at EI + 830.5/832.5).

11. Comparing selected histories showing that the actual flight was close to the planned flight up to EI + 900.

12. Using the rolling-moment-coefficient history to support findings for some of the previous eleven points.

It is recognized that there are other data (facts) and that some of these facts may become critical as an improved and more complete understanding of the demise is achieved. However, based on our understanding at this time, we believe that these twelve "critical data/events" are very important and that a demise scenario that incorporates all twelve has some credibility. The time-dependence of these twelve events will be based on the "Relation of Reentry Parameters" that are contained in the table presented in Table 1 and in Appendix A. Entry Interface (EI) occurred at GMT 13:44:09. Referring to Table 1, the reader can identify three, related early "events" that indicate anomalous behavior: the strain gage reading and the high temperatures for two thermocouples on the spar behind RCC Panel 9 (one on the clevis and one on the back face of the spar. These foreboding signs occurred by 13:49:00, with the Orbiter still approximately 1000 miles west of the California coast. The Orbiter was flying at altitudes in excess of 260,000 feet, where non-continuum effects are important in modeling the flow field and the peak convective heating has not been reached. Thus, it is believed that the initial damage that compromised the thermal protection system and that led to the demise of OV-102 was in place at the EI.

To readily access the figures and appendices of this report click on the hyperlinks located on the last page of this document.

GENERAL DISCUSSION

(1) The observation that foam particles from the external tanks impinged on the wing leading edge during launch.

A large piece of foam (debris) from the bipod area of the external tank (ET) is evident in the film of the STS-107 during launch. The trajectory of the debris, which is shown in Figure 1, indicates that the ET foam debris struck the wing leading edge 82 seconds after launch. Based on this trajectory, the likeliest area of impact was on RCC Panel 6, or slightly downstream. See Figure 2. As shown in Figure 3, RCC Panels 1 through 4 are located on the glove, which has a sweep angle of 81°. RCC Panels 5 through 7 are located on the intermediate spar, a. k. a., the transition spar. RCC Panels 8 through 19 are located on the wing spar, which is swept 45°,

Post-flight analysis of the MADS data indicated a small temperature rise in the measurement from a temperature sensor that was located behind the wing spar of RCC Panel 9. This is a possible additional piece of evidence that the damage occurred during the launch phase.

The authors believe that significant damage to the RCC panels in the vicinity RCC Panel 6 is consistent with the early thermal anomalies that were observed both in the sensors on and/or near the spar at the back of RCC Panel 9 and in some of the sensors in the left main-landing-gear wheel well. The anomalies that occurred in these two regions did not occur simultaneously, but were close in time. Thus, damage somewhere in the vicinity of RCC Panel 6 would be strategically placed to deliver hot gases that could both damage the wires on the back of the wing spar near these RCC panels and the wires on the main left-landing-gear wheel well. The hot gases from the breech in the wing leading edge would also flow down the chunnel (channel/tunnel) that exists between the RCC panels and the spar that follows the wing leading edge, producing the anomalous readings on the sensors at the spar at RCC Panel 9.

The wing-leading-edge subsystem (LESS) is shown in the sketch of Figure 4. The impact of the debris with a leading-edge RCC panel could have removed (all or part of) a T-seal or produced a hole or a crack in the RCC panel itself. In an attempt to further define the location and the extent of the debris-induced damage, NASA personnel and their contractors have been using computational fluid dynamic (CFD) codes. Additional work is needed to complete and to validate the analysis efforts, e. g., use the direct simulation Monte Carlo (DSMC) computational tools to provide an independent validation of the flow field at these low-density gas conditions. The modeling of the internal flow through the chunnel, starting with a breech of the leading-edge TPS (using the location and the nature of the breech to define the boundary conditions for a few likely initial conditions), and proceeding into the wing is a very complex task that should be completed. Of special interest is matching the computed results to the observed times for (1) the burn through of the MADS wires behind the spars, (2) the burn through of the bundle of wires that ran along the wall of the main left-landing-gear, and (3) the anomalous temperatures measured at various points inside the left main-landing-gear wheel well.

(2) Radar signatures from the second day of the mission that showed a piece of debris drifting away from the Orbiter.

Radar signatures from the second day of the STS-107 mission indicated that there was an object drifting away from the Orbiter, disappearing after a few orbits. The radar signature and the ballistic coefficient of the object were analyzed to determine what the object might be. Recent communications from personnel from the Lincoln Lab (as provided to Dr. Sheila Widnall) indicate that, in their judgment, the best match to the "data" would be a piece of a T-seal. However, the possibility exists that the impinging ET foam caused a piece of an RCC panel to be broken off. The exact configuration of the initial damage is not known.

(3) The strain-gage reading (beginning at EI + 270) and the temperature rise at two thermocouples located in the vicinity of RCC Panel 9 (beginning at EI + 290), as indicated by MADS data.

As shown in Figure 5, three sensors were located in the vicinity of RCC Panel 9: two thermocouples and a strain gage. AT GMT 13:48:39, the strain gage on the left wing spar at RCC Panel 9 starts an off-nominal increase, as indicated in Appendix A. This is only 270 seconds after EI. At this point in time, the Orbiter is located about 1000 miles west of the California coast, flying at 23,000 feet/second at an altitude in excess of 270,000 feet. Refer to Table 1. Referring to Table 1 and to Figure 6, the temperature sensed by the thermocouple on the Spar 9 Clevis starts to increase by (approximately) GMT 13:49:00, which is less than 300 seconds after EI. According to Table 1, the temperature sensed by the thermocouple on the back of Spar 9 starts to increase very rapidly with time beginning at GMT 13:51:09. Refer now to Figure 7. Signal is lost from the thermocouple on the clevis at (approximately) 55 deg F, 490 seconds after EI. At approximately 522 seconds after EI, signal is lost from the thermocouple on the back face of the spar at a temperature exceeding 240 deg F.

The authors believe that the increase in temperature of the two thermocouples that are located on or near Spar 9 was caused by hot gases entering through a breech in the thermal protection system (TPS), which occurred when the impingement of the ET foam debris damaged the leading-edge TPS. Based on the information currently available to the authors, the critical, it is their opinion that the initial damage probably occurred in the vicinity of RCC Panel 6. Hot gases from the shock layer entered through the breech in the TPS and flowed down the chunnel. Although the density of these gases is relatively low, their temperature is very high. If this is indeed the case, then these hot gases flowing through the chunnel also were destroying the intermediate spar, a. k. a., the transition spar, and parts of the wing spar. Assuming this model to be correct, the hot gases would flow through the gaps and around the edges of the insulative wrap that surrounds the sensors. Thus, convection would be added to conduction and radiation, as mechanisms contributing to the rate at which the measured temperature increases.

Based on the computed flow-field solutions by NASA and on the engineering experiences of the authors, the flow path of the ingested hot gases depends on the location and on the shape of the breech in the thermal protection system. If the initial damage were a hole in the RCC panel itself, there would be a strong component of flow outward along the chunnel and parallel to the wing leading edge, following the external streamlines. If the initial damage were a piece of T-seal, the ribs of the bounding RCC

panels would constrain the flow to the channel bounded by the ribs. This flow path is initially perpendicular to the wing leading edge. However, the high temperature gases flowing in this channel could quickly ablate the downstream rib, at which time the damage would function as a hole.

Some Observations at This Point (A)

The destruction of the spar is not the only problem caused by the hot gases flowing down the chunnel. Under normal circumstances, the locally high convective heating rates to the external surface of the RCC panels along the wing leading edge are balanced by radiation into the relatively cool cavity behind the curved RCC panels, i. e., into the chunnel volume. In addition, under normal circumstances, some energy is conducted away from the leading edge through the high temperature gradients in the reinforced carbon/carbon shell. But this is no longer possible. These hot gases flowing in the chunnel not only prevent the mechanisms for relief of the energy from the RCC panels, they create a situation where the panels are being heated from both sides. The hot gases in the chunnel prevent the energy relief from the high convective heating rates to the external surface of the RCC panels. This will strike first at the RCC panel where the convective heating from the flow in the shock layer is the greatest. As will be discussed, the shock/shock interaction pattern produced the highest convective heating rates in the vicinity of RCC Panel 9. This will be discussed in "critical data/event" #4.

The destruction of the intermediate (or transition) spar somewhere behind RCC Panels 6 through 8 provides a source for the problems soon to affect objects in the left main-landing-gear wheel well ("critical data/event" #6) and the early loss of the elevon signals, which is attributed to the wire burn through ("critical data/event" #8).

(4) The perturbations to the heating and to the surface pressures due to the interaction between the bow shock wave and the wing-leading-edge shock wave are most severe in the region of RCC Panels 8 and 9.

The bow shock wave intersects the wing-leading-edge shock wave, creating a shock/shock interaction, such as shown in Figure 8 [Ref. 1]. The interaction between the bow shock wave and the wing-leading-edge shock wave depends (among other parameters) on the gas chemistry, on the angle-of-attack, and on the sweep angle of the wing. The bow shock wave is relatively weak, so that flow in the shock layer near the wing root is supersonic and the pressure is relatively low. Far outboard, the wing-leading-edge shock wave depends on the sweep of the wing leading edge. If the leading edge is only slightly swept (as was the case for some of the early Orbiter concepts), the wing-leading-edge bow shock wave will be strong with high pressures in the downstream, subsonic flow. The low-pressure, supersonic flow inboard of the interaction adjusts to the high pressure, subsonic flow outboard of the interaction through a complex flow that contains regions of subsonic flow, of supersonic flow, impinging jets, and imbedded shock waves. See Figure 8(b). The surface of the wing leading edge that is subject to the impingement of this strong viscous/inviscid interaction may see heating rates more than an order-of-magnitude greater than the heating rates that would exist if there were no shock/shock interaction. However, in actuality, the wing-leading-edge sweep angle (for RCC Panels 8 through 18) is 45^{o}. See Figure 3. Since the wing is highly swept, the wing-leading-edge shock wave will be relatively weak with low pressures in the downstream, supersonic flow. See Figure 8(c). Both the jet and the free-shear layer that are contained in the shock/shock interaction diffuse rapidly.

As a result, the shock/shock-induced perturbation to the heating in the region affected by impinging flow is relatively small for the current Orbiter configuration, i. e., approximately twice the heating that would exist if no shock/shock interaction were present.

Convective heating rates in the interaction region of the wing leading edge have been computed for the Shuttle Orbiter. The computed heat-transfer rates that are presented in Figure 9 indicate that the interaction between bow shock wave and the wing-leading-edge shock wave causes the heating to the surface in the interaction to be approximately twice the undisturbed value and that RCC Panel 9 experiences the highest heating. Because the Orbiter is operating at an angle-of-attack of 40-degrees, the stagnation line is on the windward surface just below the apex of the leading edge. Thus, the highest convective heating to the wing-leading-edge region affects RCC Panel 9, on the lower surface, just below the leading edge. As noted in the previous paragraphs, under normal circumstances, these incident heating rates would be accommodated by radiation from the back surface of the RCC panel into the cavity and by conduction through the reinforced carbon/carbon shell, away from the stagnation line. However, as shown in the sketch of Figure 10, the hot gases flowing up the chunnel not only eliminate the ability to transfer energy away from the wing leading edge, but they produce a situation where energy is added to the RCC panel from the inside as well as from the outside. It doesn't take long before the material near the stagnation line (on the lower surface) fails, leaving relatively sharp RCC plates, exposed to the flow. Thus, the authors believe that a second breech of the thermal protection system has occurred. The authors believe that this one is most likely to be on the lower surface of RCC Panel 9 $\pm$ one panel. The authors' belief that there are two breeches to the RCC panels along the wing-leading edge is based upon not only the sensor data, but upon the Kirtland photograph, which will be discussed as "critical data/event" #10. Gases quickly flow from the high pressure region in the shock layer near the stagnation line into the chunnel, causing the destruction of the lower surface of the panel. The authors believe that this is a significant change in the Orbiter Mold Line (OML). The changes in the OML of the wing leading edge modify the vortices that emanate from this region and that impinge on the leeward fuselage. Therefore, it is associated with the start of off-nominal temperature histories at the four sensors on the left OMS Pod, which are described in "critical data/event" #5.

(5) Start of off nominal temperature histories at four sensors on left OMS Pod (beginning with lower than expected temperatures at EI + 340, followed by higher than expected temperatures at EI + 460).

Refer to "The STS-107 Mishap Investigation – Combined Master Timeline, - Baseline Corrected" that is presented in Appendix A. It is noted that, at GMT 13:49:49, which is EI + 340, "Start of off-nominal temperature trends" for "4 Left OMS Pod Surface Temps". Initially, the rise rate is cooler, when compared to previous flights of the same inclination. That is followed by a warmer-than-expected temperature trend, beginning at EI + 460. It is noted in Appendix A that the "Sensor sees a sharp increase at EI + 910 and goes erratic at EI + 940."

Even for the baseline configuration, i. e., for the configuration without any damage to wing leading edge, free-vortex-layer types of separation are produced by the flow around the fuselage chine, around the highly swept glove (sweep angle of 81^{o}) and around the transition section from the glove to the majority of the wing, which is swept 45^{o}. The resultant viscous/inviscid interactions cause locally high heating rates and high

shear forces to act on the orbital maneuvering system (OMS) pod. However, as is evident in the data presented by Neumann [Ref. 2] and reproduced in Figure 11, the heating to the OMS Pod is a function of the angle-of-attack. The correlation between the local heating and the angle-of-attack is important, since the Space Shuttle Orbiter employs ramping during entry. That is, the angle-of-attack of the Orbiter during entry is initially high, i. e., approximately 40-deg. until Mach twelve is reached. Then, it is ramped down, reaching approximately 20-deg., when the flight Mach number is four. The reader should note that there are significant differences between the heat-transfer correlation based on the wind-tunnel data and that based on the flight data. These differences can be traced, at least in part, to real-gas effects, to Reynolds-number-related effects, and/or to low-density effects.

The first author had a similar experience involving a difference between viscous/inviscid correlations based on wind-tunnel data and those based on flight-test data from the Gemini program. During the design phase of the Gemini capsule, it was assumed that the reentry aerothermodynamic environment for Gemini capsule was similar to that for the Mercury capsule. Thus, the wind-tunnel test program that was conducted during the design phase of the Gemini was somewhat limited. However, the Mercury capsule flew at an angle-of-attack of zero degrees, while the Gemini capsule reentered at an angle-of-attack of approximately 20-deg. Because the Gemini capsule flew at non-zero angle-of-attack, a vortex-induced viscous/inviscid interaction produced locally high heating rates on the conical surface in the vicinity of the umbilical fairing. The locally high heating rates produced numerous, small holes in the surface of the conical frustum of the capsule that was made of Rene 41. Once the inspection of the recovered capsule revealed the damage, a post-flight wind-tunnel test was conducted with instrumentation specifically located to obtain information about the aerothermodynamic environment in the region of perturbed flow. The wind-tunnel data revealed that locally high heating rates due to the viscous/inviscid interaction caused by the presence of the flow over the umbilical fairing. Although the wind-tunnel tests revealed the presence of and the approximate strength of the perturbations, there were considerable differences between the severity and the locations of the flight-observed damage and those based on the wind-tunnel tests. The results were similar to those of Figure 11.

By EI + 290, anomalous readings have occurred at the three sensors near Spar 9, as discussed in section relating to “critical data/event” #3. By EI + 493, anomalous data will be evident in the data from sensors in the left main-landing-gear wheel well and on the vertical side of the Orbiter. There will be a loss of the measurements from wire bundles at various locations in the wing box, beginning at EI + 487. These anomalous data indicate there was a considerable mass flow of hot gases through a large fraction of the internal wing volume.

The off-nominal temperature trends that were discussed in the first paragraph of this section (first slightly below the expected values, then above the expected values) are attributed to changes in the free-vortex shear-layer pattern that dominates the leeward flow field. The changes in the vortex pattern are due to the changes in the Outer Mold Line and to hot gases that are flowing from the internal wing volume through the vents that are located on the upper surface of the wing. The specific location of the perturbations to the surface heat-transfer and surface pressure are sensitive to the angle-of-attack, to the Reynolds number, to the density ratio across the shock wave, etc.

Flow-field computations for an Orbiter with RCC Panel 6 removed that were presented by Labbe et al. [Ref. 3] are reproduced in Figure 12. The computations that were made with the FELISA code at the Langley Research Center (NASA) assume an inviscid flow with equilibrium air in a Mach 23.8 stream. Three principal observations are associated with the removal of RCC Panel 6:

"(1) Produces negative roll and yaw moments w/small magnitude
(2) Streamlines for the damaged vehicle track inboard of baseline
(3) Resultant shock raises pressures in proximity to temp measurements".

(6) The anomalous temperature increases that occurred at various locations in the main left-landing-gear wheel well (beginning at EI + 488).

The first sign that hot gases had reached the main left-landing-gear wheel well showed up in the brake-line temperature measurements. A "bit flip" in the "LMG Brake-Line Temp D" occurred at GMT 13:52:17 [Ref. 3]. This is temperature trace M in Figure 13. Thus, this event occurred 488 seconds after EI, which is approximately three minutes after the anomalous readings in the vicinity of Spar 9 ("critical data/event" #3). While a "bit flip" may well be within the experimental uncertainty and, therefore, will not be truly indicative of a problem, the LMG Brake-Line temp D was only one of many anomalous measurements that occurred in this time frame at sensors in the vicinity of the left main-landing-gear wheel well. Referring to Table 3, three "LMG Brake Line Temps" began unusual temperature increases in the time frame GMT 13:52:17 to GMT 13:52:41. Both the temperature measurement for LMG Brake-Line Temp C, which is trace I in Figure 13, and the temperature measurement for LMG Brake-Line Temp A, which is trace G in Figure 14, exhibit anomalous increases starting at GMT 13:52:41. These three gages cover X_0 coordinates from approximately 1100 through 1200. Thus, all three sensors are aft of the tires of the LMG. Because the rate of increase for the temperatures sensed in the wheel well was relatively slow, the hot gases didn't impinge directly on these sensors. Instead, the authors believe that the hot gases entered the cavity away from the sensors and gradually heated the volume of air that resided in the wheel well. Because of the severe damage on the tire and of the aluminum residue splattered on a door latch, the authors believe that the plume of hot gases could have entered that area through a breech near RCC Panel 6.

(7) The increase in temperatures at points located on the vertical side of the fuselage, as indicated both in thermocouples on the Orbiter itself and in the temperature sensitive coatings on the wind-tunnel models tested at the Langley Research Center (beginning at EI + 493).

It is noted in Appendix A that, by GMT 13:52:52, i. e., EI + 493, unusual temperature shifts were observed in five thermocouples on the fuselage and on the upper left wing. It is noted in Table 1 that "Mid fuse bond temp starts up" at GMT 13:54:22. The location of this sensor is noted in Table 3 as X_0 = 1410. Hasselback [Ref. 4] reports that, at GMT 13:53:29, "Fuselage side surface temp increase at X_0 1000.7". Because these anomalous fuselage side-wall temperatures were given a separate mention in the time line of Appendix A, it is given a separate data/event number in this report. However, the flow phenomena that cause these anomalous are essentially those associated with the anomalous heating to the left OMS Pod, i. e., "critical data/event" #5.

Wind-tunnel data from the 20-inch Mach 6 (Air Wind Tunnel) at the Langley Research Center (NASA) that are reproduced in Figure 15 show increased heating rates

on the side of the Orbiter fuselage both for only RCC Panel 6 removed and for only RCC Panel 9 removed.

(8) Loss of all measurements from the wire bundle running along the backside of the wing spar (beginning at EI + 487) followed by the loss of measurements from the wire bundle running along the left main-landing gear wheel well, which included elevon measurements (beginning at EI + 527).

Several of the wires carrying signals from the MADS sensors (including the two temperature measurements behind RCC Panel 9, one on the clevis and one behind the spar) run behind the RCC Panel 9 area wing spar along the back of the spar, forward to the front of the wheel well (about RCC Panel 5). See Figures 16 and 17. At EI + 487, the sensors whose wires run on the back of the left wing front spar begin going off-line, indicating a burn through of the spar. Over the next 10 seconds most of these signals go off line. The last one, the bottom-most wire, goes off-line at EI + 522. Since these wires are separated by about eighteen inches in most locations, the breech, at least its vertical dimension, had to be quite large. Beginning at approximately GMT 13:52:59, which is equivalent to EI + 530, the wires in the large bundles that run along the top of the wheel well (See Figure 17 and 18) begin to go off line. The first signal to go off line was the elevon lower skin temperature. Over the next minute or so most of the signals in these wire bundles go off line. See Figure 19. This would indicate a significant amount of heat was impinging on the wires and wheel well wall. NASA has performed a number of tests to investigate the burning of wire bundles. These test demonstrated that the rapid loss of the entire wire bundle requires very hot gases, with local heat rates of 80 to 90 Btu/ft^2-sec. It is likely that the wheel well wall had been penetrated at this time, since anomalies were showing up in the temperature measurements in the left main-landing-gear wheel well. Recall that the first observed “bit flip” in the wheel well was at EI + 488. While this single “bit flip” may or may not be significant by itself, within the next one to two minutes most of the temperature sensors on the landing gear in the wheel well began to increase. Refer to the discussion of “critical data/event” #6.

This sequence raises some dilemmas that need to be addressed. First, how do we get enough heat on the wheel well to burn the wires, but yet the sensors in the wheel well stay on line until the loss of the Orbiter and the temperatures only go up about 40^oF. Second, the hole through the spar has to be large enough (> 18 inches tall) to take out all the wires, creating a large path for the hot gases to go into the wing interior, yet much of the aluminum wing structure stays intact for another 8 minutes. One explanation could be that a T-seal (or portion of a T-seal) missing. With a T-seal the impinging jet would be narrow, but tall enough to cut all the MADS wires. It could take out the vertical array of wires without the massive heat a “circular hole” would deliver. Also, it would seem that the breech in the spar should be near where the wire bundles (MADS and OI) are close together so the required heat would be minimized. This would favor a breech through a lower number RCC panel. However two strain gages on the front of the wheel well did not go off-line (See Figure 18). This would tend to rule out RCC Panel 5, which is ahead of the front wheel well wall. If the initial damage were to a T-seal (or maybe created a hole just upstream of an RCC rib), the hole through the spar could be smaller and still burn a vertical array of wires. Interestingly enough, such a damage configuration would result in initial flow perpendicular to the spar and cut wires. After 2 to 3 minutes, the very hot gases impinging on the downstream edge of the slot would burn through the RCC rib. At this point the hot gases would tend to flow down the chunnel, damaging the downstream RCC panels and the spar.

(9) The observations regarding the damage to the wing leading edge, as determined from the recovered debris.

Many members of the Board and support staff have spent considerable time in Florida examining the recovered debris. Experts such as Jim Arnold, Howard Goldstein, Pat Goodman, Greg Kovacs, Mark Tanner, and Don Rigali have spent considerable time and effort analyzing the recovered debris. The present authors are not as knowledgeable as many others on the detailed interpretation of the reconstructed wing leading edge. Therefore, our conclusions rely on the photographs, reports, and oral feedback from these experts. Photographs of the reconstructed wing-leading-edge panels, RCC Panels 5 through 11, are presented in Figures 20(a), 20(b), and 20(c). Note that very little of the bottoms (windward surfaces) of RCC Panels 6 through 9 have been recovered. The authors interpret the damage pattern to RCC Panels 6 through 9, as supporting their belief that the foam-induced damage was centered on RCC Panel 6 and the subsequent damage caused by the blockage-of-relief/additional-heating from the chunnel gases led to the loss of most of RCC Panel 9. Because RCC Panel 9 is in the most severe region of the baseline shock/shock interaction region, it would be expected to suffer the most damage. Thus, we believe that the subsequent loss of RCC Panel 9 left two regions where substantial damage had occurred to the wing-leading-edge RCC panels relatively early. Of course, the absence of debris could mean simply that the debris has not been found. It appears that significant fractions of the upper section of RCC Panels 7 and 8 have been recovered. Thus, it appears that there was a surviving section of RCC panel(s) between the two gaps. This is consistent with the authors' belief that, by the time of the Kirtland photograph, there were two distinct notches in the wing leading edge, which were caused by the loss of a substantial amount of RCC Panel 6 (+/- one panel) and RCC Panel 9 (+/- one panel). Between these "missing" panels, a piece of the wing leading edge (what we believe to be the surviving pieces of RCC Panels 7 and 8) remains in place.

The experts report that there is a lot of unique damage in the vicinity of RCC Panels 8 and 9, noting that there is considerable slag deposited on the inner surfaces of the upper portions of the recovered panels. The relative metallic deposition on left wing materials is presented in Figure 21. Note that the metallic deposition is "heavy" to "very heavy" behind RCC Panels 7, 8, 9, and 10. Since the predominate flow stream will be up and out along the chunnel, this pattern would be consistent with an initial breech in the vicinity of RCC Panel 6 +/-1 panel with the hot gas plume impinging on the spar behind RCC Panels 7 and 8, causing splatter on the material in this area.

The authors believe the recovered portions of RCC Panels 6 through 10 are reasonably consistent with the demise history of the panels that will apply to "critical data/event" #10. Moving circumferentially around the wing leading edge in an x-y plane, the most severe convective heating occurred in the vicinity of the stagnation line in the shock/shock-interaction region, which is most severe for RCC Panel 9 $\pm$ one panel. See Figure 9. The burn through started at the stagnation line and proceeded to eat away the RCC shell in either direction. Thus, it is not surprising that the lower surface has not been found for any of these RCC panels. The hot gases flowing through the chunnel from the original ET foam-induced breech to the thermal protection system (TPS), which occurred in the vicinity of RCC Panel 6 +/-1 panel, ate away at numerous metal surfaces, depositing the residue as slag on the surviving inner surfaces of the leading edge TPS elements.

It would be reasonable to expect that, if any portion of an RCC panel were recovered, it would be upper portion of the panel. The lower portion (which is the windward portion and, therefore subjected to the greatest convective heating) of the panel may be destroyed during the expanding destruction of the reinforced carbon/carbon shell. Referring to Table 2 and Figure 20(c), the upper portions of RCC Panels 7 and 8 on the left wing have been recovered. Only the edges of the upper portion of RCC Panel 9 have been recovered. As of the date of this writing, the lower portions of these three RCC panels have not been found.

Some Observations at this Point (B)

Referring to the timeline record presented in Table 1 for the flight STS-107 of OV-102, the first debris was seen leaving the Orbiter at GMT 13:53:44. Hot gases have been entering through a breech, or breeches, that occurred in the vicinity of RCC Panels 6 though 10. Sensor measurements on the spar behind RCC Panel 9 indicate anomalies starting at approximately GMT 13:48:39, which is 270 seconds after EI. Temperatures sensed at various points in the LMG brake line exhibit anomalous behavior, starting at GMT 13:52:17 (or slightly later). Thus, the anomalous temperature measurements from the main left-landing-gear wheel well started approximately 488 seconds after EI.

Note that "critical data/events" # 3 and #5 through #9 take place over several minutes in time, affecting first sensors at the spar behind RCC Panel 9, which is relatively close to the wing leading edge, and then, approximately three minutes later, affecting brake line temperatures in the LMG wheel well. This pattern is consistent with a damage model that starts with a foam-impact-induced breech near RCC Panel 6 ± one panel. Hot gases flowing through the chunnel not only block the path for relieving the relatively high heating rates to the external surface of the RCC panels in the vicinity of the shock/shock interaction, but cause these critical panels to be heated from both sides. Because the shock/shock interaction to the baseline configuration produces relatively high heating rates centered in the vicinity of RCC Panel 9 (refer to Figure 9), the internal flow next creates catastrophic damage to the TPS in this region. Thus, the RCC panels in this region undergo growing damage, providing a second breech to the TPS. As noted earlier, at this point in time during reentry, there has been a significant change to the Orbiter Mold Line (OML).

Note that it is the authors' opinion that the limited data available to the authors at this time does not rule out the possibility that the initial foam-impact-induced breech might have affected an RCC panel downstream of RCC Panel 6. However, the Kirtland photograph, which will be discussed in the next section, indicates to us that there are two gaps in the wing leading edge. Regardless of where the initial breech of the wing leading edge occurred, the locally high pressures due to the shock/shock interaction that exist for the baseline Orbiter configuration are greatest on the surface of RCC Panel 9 +/- one panel. These pressures drive the hot gases into the wing volume, contributing to the heating to those gages on the spar behind RCC Panel 9. Then, within a few minutes, the gases break through the spar and the LMG wheel-well wall. Damage to the Orbiter is growing rapidly. The first five debris events (refer to Table 3) occurred in the time GMT 13:53:44 to 13:54:11. The demise of one or more RCC panels changes the Orbiter Mold Line (OML) geometry of the wing leading edge. Instead of encountering a rounded leading edge with gradually changing wing-leading-edge sweep angles, the

oncoming flow sees cavities or notches in the wing leading edge, flat faces of (what is left of) the spars, metal surfaces of high catalycity, etc. See Figure 22. Locally strong shock waves that are imbedded in the viscous/inviscid interaction change the nature of the interaction to one more like that of Figure 8(b). A significant increase occurs to the perturbations in heating to the erose leading edge formed by the damage to/loss of those RCC panels in the "transition zone", e. g., RCC Panels 6 through 9. All of this, occurs with the Orbiter flying at velocities in excess of 22,000 feet/second (Mach 22.5) and at an altitude of 227,000 feet where the flow is a continuum and the aerothermodynamic environment is severe.

The scenario now becomes one in which the damage accelerates dramatically.

(10) The modifications to the shock/shock interaction flow field of "critical data/event" #4, as developed based on the developing damage scenario and correlated against the Kirtland photograph, i. e., observations by personnel from the Starfire Optical Range (at EI + 830.5/832.5).

As noted in the previous paragraphs, debris events 1 through 5 take place from GMT 13:53:44 to GMT 54:11. See Tables 1 and 3. A number of tiles and/or pieces of individual RCC panels along the leading edge have been ablated, or lost. See Figures 20(a) through 20(c) and the "The Content of Left RCC Panels" in Table 2. Consistent with our premise, let us assume that there are at two gaps due to "missing" RCC panels from the wing leading edge. Missing is in quotes because parts of the panels are probably still in place. Furthermore, each notch may represent one or more RCC panels. Recall from the previous discussion that the initial, critical, foam-impingement-induced damage possibly affected RCC Panel 6 ± one panel. The early and rapid responses of the three sensors near the spar behind RCC Panel 9 led to the postulation that hot gases were flowing through the chunnel. The significant amount of metallic deposits on left-wing materials presented in Figure 21 further supports the contention that damage to RCC Panel 6 was the initial breech. Downstream, leading edge RCC panels were being heated from both sides, with disastrous effects. The most disastrous were to the RCC panels located where the shock/shock interaction heating was the greatest, RCC Panel 9. Thus, based on the previous discussion, we will assume that the two notches are centered on RCC Panel 6 and on RCC Panel 9. Refer to Figure 22.

As shown in the sketch of Figure 23, the loss of these segments along the wing leading edge present the oncoming flow with notches that contained flat faces, forward-facing corners, etc., instead of the gradually changing sweep angle and the rounded nose of the undamaged wing leading edge of the Orbiter. Locally strong shock waves, i. e., shock waves that are perpendicular to the oncoming flow, occur for each notch. A portion of each shock wave is normal to the oncoming flow, but only for a short distance. The notch-induced shock waves quickly curve away as the flow follows the RCC surface downstream of the corner. Thus, the shock shape has a "bubble-like" appearance in the plane of the paper.

The shock-layer structure postulated for each notch in the sketch of Figure 23 is similar to that obtained during the Mach 6 wind-tunnel tests that were conducted at the Langley Research Center. See Figure 24. Consider the curved shock wave associated with the notch created by the removal of RCC Panel 9 from the wind-tunnel model. The trace of the shock wave nearest the wing root, i. e., the trace that extends into the notch produced by the missing RCC Panel 9 is normal to the oncoming flow. Thus, the flow

immediately downstream of the normal shock wave is subsonic. As the shock wave curves, it becomes weaker and the flow immediately downstream of the shock wave is supersonic. Because the shock wave is curved, there is considerable vorticity in the shock layer flow approaching the wing leading edge. The curved shock wave associated with the notch of RCC Panel 6 would exhibit similar features. Furthermore, when these two curved shock waves intersect for this high angle-of-attack configuration, they create an extremely complex flow field.

Consider next the flow of the air in the shock layer just ahead of the wing leading edge. The density of the air in the shock layer will be greatest in the shock-layer flow downstream of the normal portions of the shock wave. The large density gradients that occur in the shock layer flow would cause light rays from a distant source on the far side of the vehicle to be bent as they pass through the shock layer. Light rays would bend due to the large second derivatives in the density of the air in the shock layer, producing dark areas in a photograph of the flow. This phenomenon is similar to the shadowgraph technique, which is used to visualize the shock-wave structure in a wind-tunnel flow. The stand-off distance from the shock wave to the vehicle surface is relatively small for these hypersonic flows. Thus, the shock layer flow in the shadowgraph may appear as a dark region in the plane of the photograph. The reader should note that this is a two-dimensional trace of a three-dimensional phenomenon.

A photograph of the Orbiter in flight was taken by personnel at the Starfire Optical Range is presented in Figure 25. This is called the Kirtland photograph. It was taken at EI + 830.5/832.5, which is just less than two minutes before the loss of signal. Note the similarity between the notch-induced shock-wave structure that the authors postulate for the flow near the wing root (refer to Figure 23) and the darkened area in the Kirtland photograph (refer to Figure 25), which contains two bubbles in the darkened area near the intersection of the wing with the fuselage. Many investigators have tried to define the place of the Orbiter within the darkened area. Two examples of these attempts are presented in Figures 26 and 27. Although the present authors do not necessarily agree with the phenomenological models proposed for these two figures, they do support our belief that damage to the wing-leading edge in the form of missing RCC panels produces a multiply-curved shock structure. The existence of two notches along the wing leading edge produces a shock-layer structure, which is consistent with the present authors' interpretation of the Kirtland photograph.

Assume that the breech of the wing leading edge through the loss of "two" RCC panels occurred near GMT 13:54:00, i. e., the time of debris events one through five. "Two" is in quotes, because the possibility exists that portions of adjacent RCC panels may also be missing during this time frame. Why does the darkened region in the Kirtland photograph, which was taken at GMT 13:57:59.5, which was approximately 240 seconds later, still correlate with the authors' model of the notch-induced perturbed flow? The authors believe that, while there is a considerable mass of hot gases flowing through the wing box, there is a considerable thermal mass available to absorb the energy in these hot gases. Thus, it takes awhile for the damage to the structures in the internal wing volume to reach the critical limit, where the left wing will break off. This occurs somewhere between the time of the Kirtland photograph (EI + 830.5/832.5) and the LOS (EI + 923).

(11) Comparing selected histories showing that the actual flight was close to the planned flight up to EI + 900.

Beginning at EI + 270 and continuing through EI + 923, which corresponded to LOS, the damage to OV-102 grows continuously. Breeches along the wing leading edge allow hot gases to flow through large portions of the internal wing volume, destroying structures in its path. Venting gases and the changes to the OML modify the vortical flow over the leeward surfaces of the Orbiter. Nevertheless, the "actual, or as flown trajectory" was very close to the "planned trajectory". Referring to Figure 28, the velocity history for the actual trajectory follows closely that for the planned trajectory through EI + 923. A similar comparison for the altitude history would produce the same degree of agreement.

It is noted in Appendix A that angle-of-attack modulation becomes active at EI + 562. "Entry Guidance enables limited delta angle of attack commands from the reference angle of attack to promote improved convergence to the reference drag profile". Referring to Figure 29, the reader can see that the "actual, or as-flown" angle-of-attack history follows "reasonably well" the "planned" angle-of-attack history until after EI + 900. The actual angle-of-attack was usually within one degree of the planned flight angle-of-attack.

Thus, despite the growing damage, many of the flight performance parameters remain close to nominal up to this time. At some time after (approximately) EI + 860, with the Orbiter over Texas, a substantial portion of the left wing probably broke away. From then on, there were a plethora of indicators of trouble.

(12) Using the rolling-moment-coefficient history to support findings for some of the previous eleven points.

The delta rolling moment history is presented in Figure 30. The strong oscillatory variations of the delta rolling moments that occur before GMT 13:50:00 were attributed to experimental uncertainty from the outset, as noted by Labbe et al. [Ref. 3]. From GMT 13:50:00 through GMT 13:53:00, the delta rolling moment was relatively constant and negative. The magnitude is within the experimental uncertainty. Furthermore, additional review of these data indicated that there had been flight-to-flight variations of similar magnitude from previous flights. Winds were offered as another factor that could have affected the data in this time frame. Because of these three factors, the authors have assumed that none of the delta rolling moment data for times before GMT 13:53:00 are definitive.

From GMT 13:53:00 to GMT 13:54:00, the delta rolling moments are negative (left-wing down) and becoming more negative with time. See Figure 30. In the same time frame are the first five debris events. Recall that, for the flow field that was computed for the Orbiter with RCC Panel 6 missing, there were negative rolling moments of small magnitude. See Figure 12.

Research activities have been conducted by personnel at the Langley Research Center (NASA) to determine the flow field of the Shuttle Orbiter at an angle-of-attack of 40^{o}. Notches in the wing leading edge simulated missing RCC panels. The Mach 24.2 flow field was computed assuming that the Orbiter was missing RCC Panel 9 and that the air was in thermochemical equilibrium. Surface pressures for this computed flow

field are presented in the lower right-hand figure of Figure 31. Streamwise streaks of high pressure are associated with the vortices from the shock interactions and from the flow around the notches. The effect of the vortices are also exhibited in the streamwise streaks of high heating that bound the large area of lower left wing surface where the notch has perturbed the heating. See the lower left-hand figure of Figure 31.

High pressures act at the notch left by the loss of RCC Panel 9. The probable loss of a good portion of the spar behind that RCC panel provides a path for the hot gases to create devastation to the structures in large areas of the internal wing volume. Although temperature measurements in the LMG wheel well have been indicating problems for over two minutes, the damage to the wing front spar and internal struts is increasing. The timeline presented in Table 1 indicates that, during the same time frame that first five debris events occur. It is likely the upper interior wing honeycomb surface is being heated above the RTV (tile bonding adhesive) failure limit and the tiles are coming off. It is also possible a larger section of the honeycomb aluminum burns or comes lose which could correspond to the flash (burning of the vaporized aluminum) observed in this time period.

As the internal wing structure (spar and struts) melts, the dynamic pressure on the lower wing surface would likely cause some wing flexure, bending up or dimpling of the lower wing. Loss of the internal wing structure would put added loading on the remaining RCC panels causing them to break, consistent with observed panel tops cracked at the apex. A bent spanner beam was also found. These phenomena also contribute to the explanation of the increasingly positive rolling moment observed.

CONCLUDING REMARKS

This document develops a plausible scenario for the demise of the Shuttle Columbia based on what the authors judge to be 12 critical pieces of data. While there is lot still unknown and much we'll never know, the authors believe there is sufficient collaborating evidence to support the following conclusions:

1. At 82 seconds into the launch, the ET-foam debris strikes the wing, damaging the leading edge. For reasons discussed in the main body of the report, the authors believe the initial breech was in the vicinity of RCC Panel 6 ± one panel. This also would mean the breech was present at start of reentry.

2. Hot gases entering a breech near RCC Panel 6 have several negative effects. First, hot gases flow down the chunnel, causing the MADS sensors near spar 9 to have anomalous responses early in the entry. The slag and other melting metallic components are splattered onto the surfaces behind RCC Panels 7 through 10. See Figure 21. Second, the incoming plume impinges on the spar, eventually burning a hole. Third, the hot gases in the chunnel reduced the heat rejection capability of the RCC panels downstream (outboard) of RCC Panel 6. Since these RCC panels are in the region where the baseline shock/shock interaction pattern is most severe, a second breech in the TPS occurs near RCC Panel 9 ± one panel. Soon other RCC panels in the vicinity experience significant ablation. See Figure 20(c).

3. The hole through the spar has some defining characteristics. It has to burn all 4 MADS wire bundles on the back of the spar (making it about 18 inches high), yet focus enough heat on the OI (telemetry) wire bundles several feet away on the top of the wheel well to burn them quickly. A missing T-seal (or a portion thereof) near RCC Panel 6 ± one panel would allow a concentrated slit of hot gases to cut the wire bundles, without depositing heat to a large internal volume in the wheel well. Since the temperature sensors in the wheel well all increase together, but at a very slow rate (about 8 degrees per minute), the plume can't be impinging directly on these temperature sensors. Within a few minutes, the slit jet will change to a "circular" hole as the downstream rib burns through. The change in the geometry of the breech causes more of the hot gases to flow down the chunnel.

4. Damaged panels near RCC Panels 6 and 9 would explain the OMS-Pod heating transients because of the perturbation to the flow over the wing. This behavior is consistent with studies being conducted at the Langley Research Center (LaRC). Notches at two locations along the wing leading edge appear as a double hump in the leading edge flow field that is captured in the Kirtland photograph, which was taken when the Orbiter was visible to the Starfire Optical Range,

5. The debris damage shows a lot of unique damage in the region of RCC Panels 8 and 9. This is consistent with a secondary burn through in this max-heat area after hot gases get in the chunnel. The fact that much of the bottom panels in region 6 to 10 are missing would be consistent with burn through on the bottom high heat area. Probably first occurring at the shock-shock interaction centered on RCC Panel 9, but eventually affecting RCC Panels from 6 to 10. The tire in

the left wheel well shows unique burning, as does one of the main gear up-lock parts. This would be consistent with a jet originating behind RCC Panel 6 and burning through the wheel well near the tire. The tire would protect the temperature sensors in the wheel well from being directly hit and, as a good insulator, help diffuse the heat for a while giving in a more uniform heat up rate in the wheel well.

6. The small initial decrease in rolling moment is consistent with LaRC wind tunnel test with "missing" RCC panels. The hot gases will penetrate into the wing front spar region and the wing internal structure. As this wing support structure is destroyed the lower wing surface will begin to flex upward under the increasing dynamic pressure load as the atmospheric density increases. The changing shape could explain the continuing increase in roll moment up until the loss of signal at about EI + 923.

While there is much that will never be known about the demise the authors judge the scenario developed in this paper is reasonable and may best correlate with the available aero, thermal, debris, and timeline. At the time of this report, NASA has not yet completed an integrated Aerothermal-structural analysis starting with a breech in the vicinity of RCC Panel 6.

REFERENCES

[1] J. J. Bertin, Hypersonic Aerothermodynamics, AIAA Education Series, Washington, D. C., 1994.

[2] R. D. Neumann, "Defining the Aerothermodynamic Methodology", J. J. Bertin, R. Glowinski, and J. Periaux (eds.), Hypersonics, Volume I: Defining the Hypersonic Environment, Birkhaeuser Boston, Boston, 1989.

[3] S. Labbe, J. Caram, and C. Madden, "CAIB Public Hearing", Tuesday, 18 March 2003.

[4] M. Hasselbeck, "Preliminary Conclusions Based on MADS Data", April 2003.

To link to the figures and appendices please click on the following hyperlinks:

To see figures click on 2 Fatal Reentry of STS107 Data and Observations.ppt

To see appendix click on 3 Timeline-STS-107-REV17-BASELINE.xls

Figures for

Using the Data and Observations from Flight STS-107 to Explain the Fatal Reentry of the Columbia Orbiter OV-102

Relationship of reentry Parameters

Order of Magnitude Estimates Only!

Values from NASA briefs and text books
Prep. By Jim Smiley X7545

Rev 5
4/30/03

GMT	Time from EI min	Altitude Feet	Air Density slugs/ft3	Atmos Press #/sqft	Dynam Press #/sq ft	Equiv Sea L speed Mile/hr	Heat Rate analys Btu ft2sec	LE Temp analys deg-F	Mach	Vel ft/sec	Location	Key Entry Events Rev 14	Debris Events	Number Dens Mole/ft3 Later	Altitude Miles	Km	Mean free path Path lambda ft Inf gas reg	Lambda inches Free space	Mean free path lambda Layer Lmda fr/20 Later	no dens Free air	MAX KE 1/2pv*v*v per ft2 Btu/ft2sec	Air Flow lbm/ft2sec	Oxygen Flow rhoxvx.23 lbm/sqft-sec	Max Aluminum Burn rate if hot enou Mils per sqft-sec	Heat of Combustion if hot enough Btu per sqft-sec
13:44:00	0	400000	5.4E-11	~0	0	0	0	0	24.6	23000		13:44:09 Entry Interface			76	126	6	72		1.73E+16	0	4.0E-05	9.1E-06		0.00
13:44:15																									
13:44:30	:30						1	100														1.7E-04			
13:44:45																									
13:45:00	1:00						1	200														3.0E-04			
13:45:15																									
13:45:30	1:30						2	350														4.2E-04			
13:45:45																									
13:46:00	2:00	340000	7.5E-10		0	9	3	500		22920					64	107	0.700	8.405		2.42E+17		5.5E-04	1.3E-04	0.01	1.86
13:46:15																									
13:46:30	2:30	327000					7	800		22900					62	103						1.8E-03			
13:46:45																									
13:47:00	3:00	314000					10	1100		22890					59	99						3.0E-03			
13:47:15																									
13:47:30	3:30	301000					15	1300		22880					57	95						4.2E-03			
13:47:45																									
13:48:00	4:00	288000	7.4E-09	~0	2	28	22	1500	24.7	22850					55	91	0.071	0.853		2.38E+18	57	5.4E-03	1.3E-03	0.10	18.26
13:48:15																									
13:48:30	4:30	274000	1.4E-08	0.01	4	38	30	1750		23050					52	86	0.038	0.461		4.42E+18	108	1.0E-02	2.3E-03	0.19	34.10
13:48:45																									
13:49:00	5:00	260000	2.5E-08	0.021	7	52	36	2000	24.6	23100		RCC-9 Clevis heating			49	82	0.021	0.249		8.17E+18	202	1.9E-02	4.3E-03	0.35	63.27
13:49:15																									
13:49:30	5:30	256000	3.0E-08	0.030	8	56	42	2200		23050					48	81	0.017	0.209		9.75E+18	239	2.2E-02	5.2E-03	0.41	75.28
13:49:45																									
13:50:00	6:00	251500	3.7E-08	0.040	10	62	46	2400		23000					48	79	0.014	0.171		1.19E+19	290	2.7E-02	6.3E-03	0.50	91.57
13:50:15																									
13:50:30	6:30	247000	7.4E-08	0.051	20	88	52	2550		22950					47	78	0.007	0.085		2.38E+19	576	5.4E-02	1.3E-02	1.01	182.91
13:50:45												Start of peak heating													
13:51:00	7:00	243000	8.8E-08	0.058	23	95	55	2700	24.1	22900		RCC 9 Spar heating			46	77	0.006	0.072		2.82E+19	679	6.4E-02	1.5E-02	1.19	216.39
13:51:15																									
13:51:30	7:30	239000	1.0E-07	0.063	27	103	57	2750		22825					45	75	0.005	0.061		3.34E+19	797	7.6E-02	1.8E-02	1.41	255.73
13:51:45												51:46 Inertial Beta goes neg-stays neg													
13:52:00	8:00	236000	1.3E-07	0.080	33	113	58	2800	23.6	22750	300 w calif	52:05 first off nominal aero signal			45	74	0.004	0.050		4.04E+19	953	9.2E-02	2.1E-02	1.69	307.93
13:52:15												52:17 Brake line temp start to rise													
13:52:30	8:30	234800	1.3E-07	0.085	33	114	60	2800		22600		52:32 Supply H2O temp rise			44	74	0.004	0.049		4.18E+19	967	9.4E-02	2.2E-02	1.74	316.51
13:52:45												52:59 Elevon Lower skin Temp OSL													
13:53:00	9:00	233600	1.4E-07	0.089	36	119	62	2800	23.3	22500		53:01 First clear Off line roll moment			44	74	0.004	0.044		4.57E+19	1044	1.0E-01	2.4E-02	1.89	344.77
13:53:15												53:10 Hyd left OB/ Inbd elev OSL													
13:53:30	9:30	231000	1.5E-07	0.102	38	122	63	2850	23	22400	Calif coast	53:36 Inbd Elevon temp OSL			44	73	0.003	0.042		4.88E+19	1099	1.1E-01	2.5E-02	2.01	366.12
13:53:45												53:44 First debris leaves orbiter	# 1 to												
13:54:00	10:00	229000	1.7E-07	0.112	41	127	64	2900		22250		54:10 LG brake/strut temp up	#5		43	72	0.003	0.038		5.32E+19	1174	1.2E-01	2.7E-02	2.18	396.59
13:54:15												54:20 Slow aileron trim change													
13:54:30	10:30	227000	1.8E-07	0.121	44	132	64	2900	22.5	22100	CA/NV Bord	54:22 Mid fuse bond temp starts up	#6		43	72	0.003	0.035		5.79E+19	1253	1.3E-01	2.9E-02	2.36	428.95
13:54:45												54:33 Bright flash seen in video	Flash 1												
13:55:00	11:00	224800	1.9E-07	0.133	46	134	64	2900		21700			# 7 to		43	71	0.003	0.033		6.23E+19	1276	1.3E-01	3.1E-02	2.49	453.10
13:55:15													#10												
13:55:30	11:30	223500	2.1E-07	0.144	47	135	64	2900		21300	NV/UT Bord		# 11 to		42	71	0.003	0.031		6.61E+19	1281	1.4E-01	3.2E-02	2.59	471.86
13:55:45		222800	2.1E-07	0.150					21.6	21000		55:41 Mid Fus sill T start off N	#15		42	70	0.002	0.030		6.86E+19	1273	1.4E-01	3.3E-02	2.65	482.68
13:56:00	12:00	222000	2.3E-07	0.158	50	140	64	2900		20850		56:03 Wing temp trend down			42	70	0.002	0.027		7.41E+19	1346	1.5E-01	3.5E-02	2.84	517.47
13:56:15												56:16 temp in LMG all up													
13:56:30	12:30	220000	2.4E-07	0.171	51	142	64	2900		20780		56:30 Roll Reversal Initiated			42	69	0.002	0.027		7.60E+19	1367	1.6E-01	3.6E-02	2.91	529.13
13:56:45																									
13:57:00	13:00	218000	2.6E-07	0.186	56	148	64	2900	20.7	20700	AZ/NM bord	56:55 Roll reversal comp			41	69	0.002	0.024		8.36E+19	1486	1.7E-01	4.0E-02	3.19	579.80
13:57:15												57:19 Tire press small rise	#16												
13:57:30	13:30	215500	2.9E-07	0.190	61	155	64	2900		20350		57:28 Wing temp off line			41	68	0.002	0.022		9.42E+19	1592	1.9E-01	4.4E-02	3.53	642.54
13:57:45												57:54 Sys 2 LH Brake vlv temp inc	Flare 1			0									
13:58:00	14:00	213000	3.4E-07	0.233	69	164	63	2900	19.9	20000	NM	58:09 Sign chang e yaw and roll	Flare 2		40	67	0.002	0.018		1.10E+20	1767	2.2E-01	5.1E-02	4.06	738.44
13:58:15																0									
13:58:30	14:30	208000	3.9E-07	0.296	73	169	62	2850	19.3	19400	Littlefield	58:32Tire temp and press OSL			39	66	0.001	0.016		1.24E+20	1818	2.4E-01	5.5E-02	4.44	807.58
13:58:45																0									
13:59:00	15:00	204000	4.5E-07	0.341	81	178	60	2800	18.6	18900	Lubbock	59:06 LMG Down lock indication			39	64	0.001	0.014		1.45E+20	1960	2.7E-01	6.3E-02	5.04	917.09
13:59:15																0									
13:59:30	15:30	200700	4.8E-07	0.381	83	180	59	2800		18600		59:33 Two yaw jets firing			38	63	0.001	0.013		1.54E+20	1985	2.9E-01	6.6E-02	5.27	959.23
13:59:45											Dallas Tx	Growth in Bank attitude error				0									
14:00:00	16:00	200000	5.0E-07	0.400	84	181	58	2800		18300		Loss of all signals			38	63	0.001	0.013		1.60E+20	1969	2.9E-01	6.7E-02	5.40	983.08

CA-000112

2 Fatal Reentry of STS107 Data and Observations.ppt

CAB068-0201

Table 2

Content of Left RCC Panels

	Lower Closeout Panel	Lower RCC Panel	Upper RCC Panel	Upper Closeout Panel
1	X	X	X	X
2	X	X	X	
3	X		X	X
4	X		X	
5			X	X
6	X			X
7	X		X	
8	X Tiles Only		X	
9	X Tiles Only		X Edges Only	
10	X			
11	X			
12				
13		X		X
14		X	X	X
15	X	X	X	X
16	X	X	X	
17			X	
18		X		
19		X		
20				
21		X		
22	X	X		

CA-000112

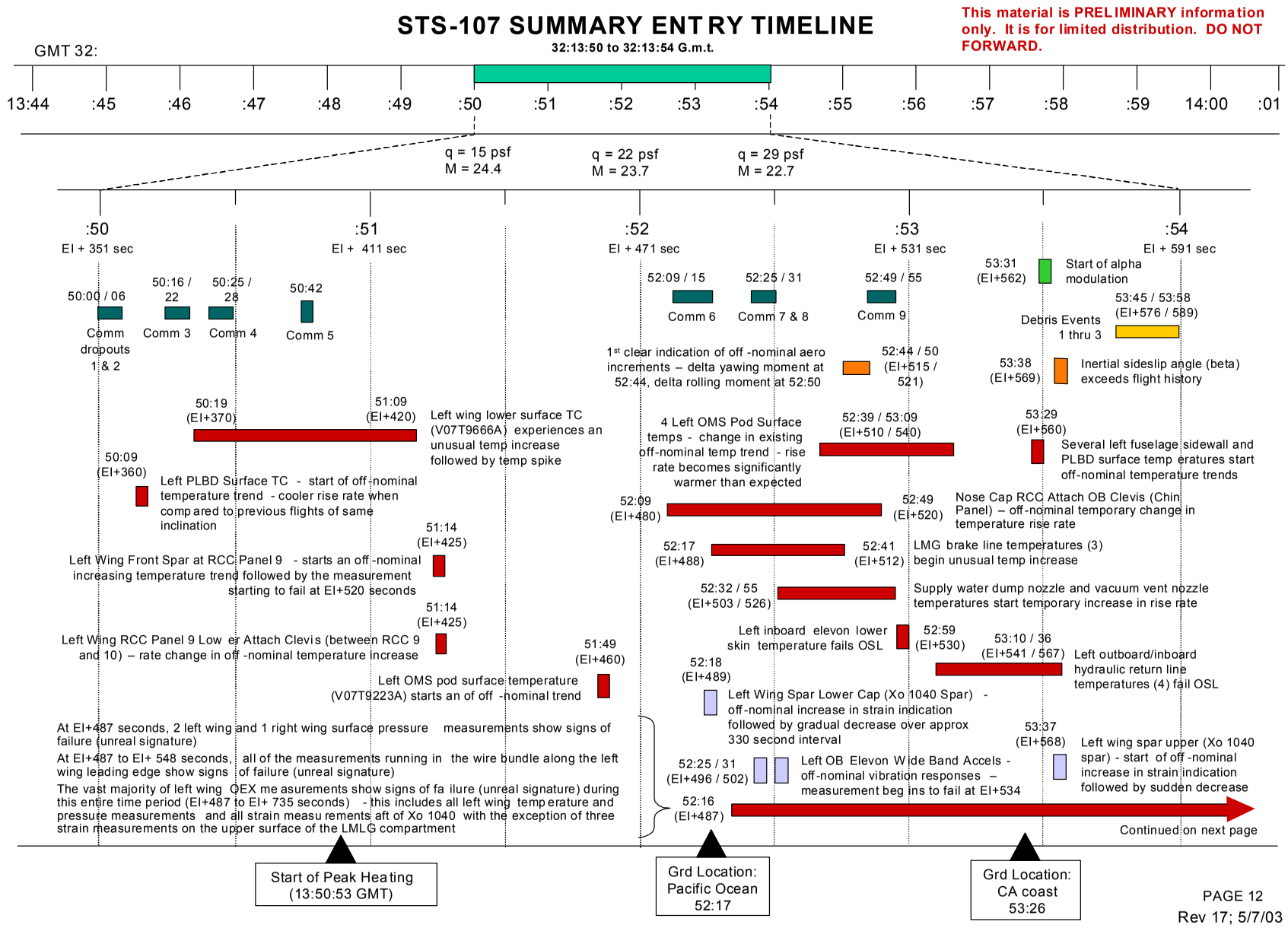

CA-000112

2 Fatal Reentry of STS107 Data and Observations.ppt

CAB068-0203

Figure 1

Ascent Debris Trajectory

- **Solid cylindrical protrusions were created through the debris locations in each view**

ET208 Camera Frame

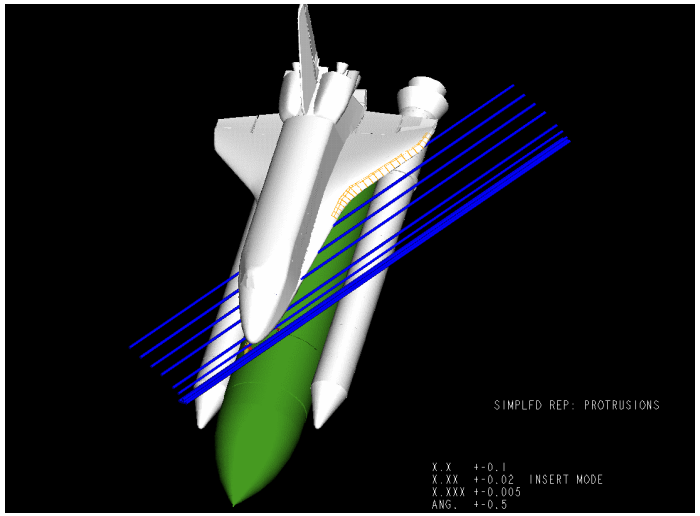

Trimetric View

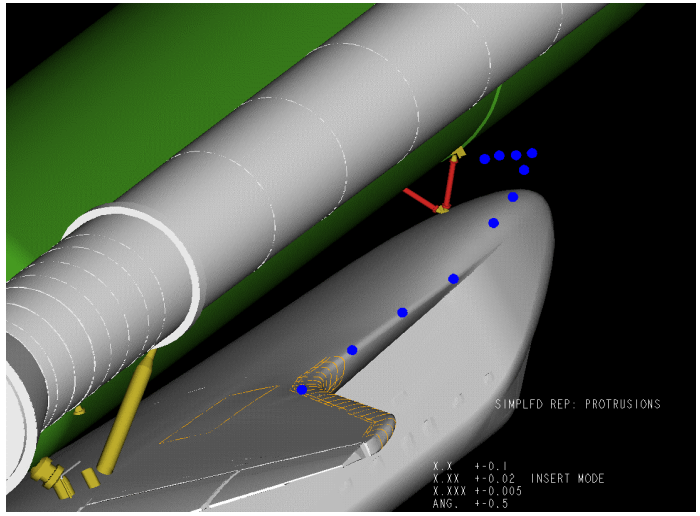

ET208 Camera View

Projection of Debris Trajectory onto Left Wing

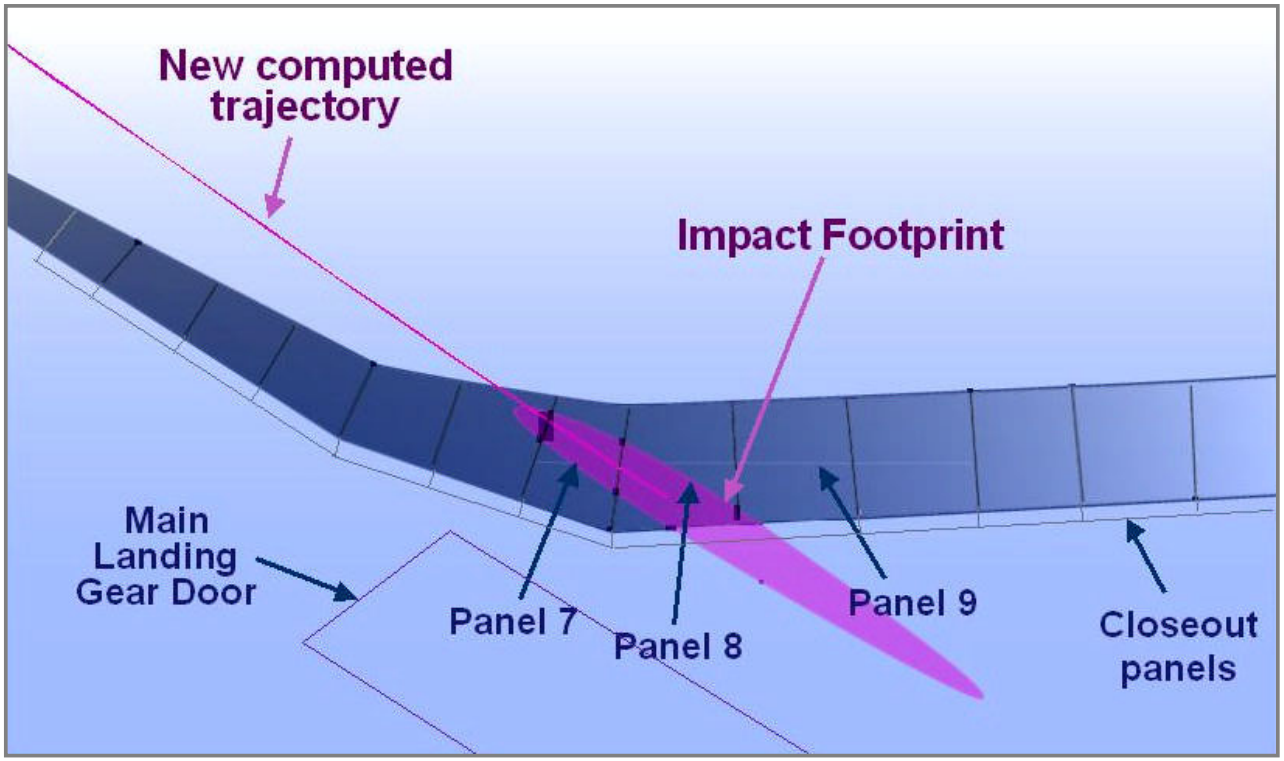

- Centerline of one-foot diameter trajectory "pipe" intersects the wing at approximately RCC panel 8, with the most likely foam impact predicted along panels 7 and 8

Figure 3

Left Wing Orientation

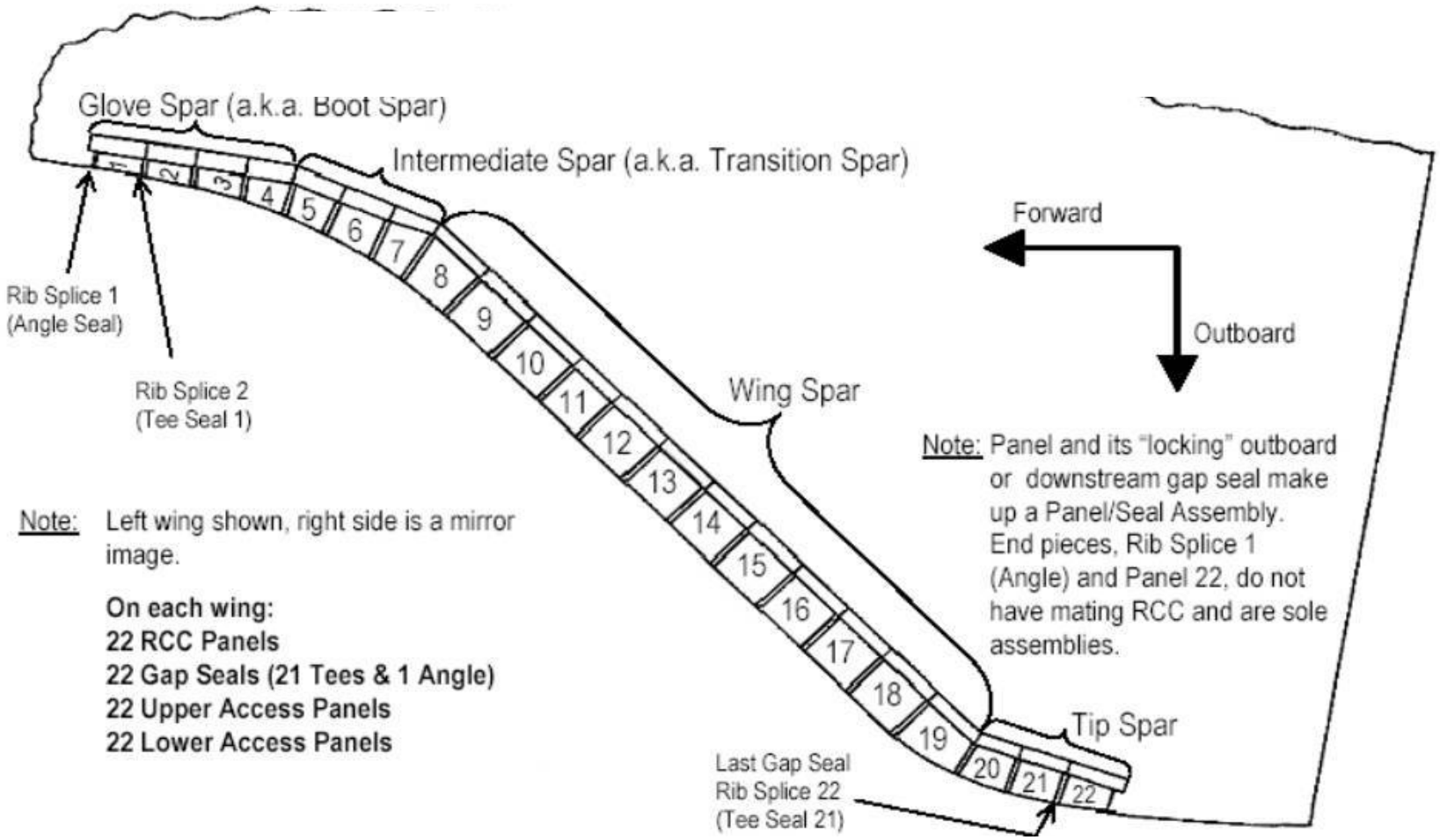

CA-000112

Left Wing Leading Edge

- Wing Leading Edge Subsystem (LESS) comprised of RCC panels, T-Seals, Upper and Lower Thermal Barriers, and associated mounting hardware

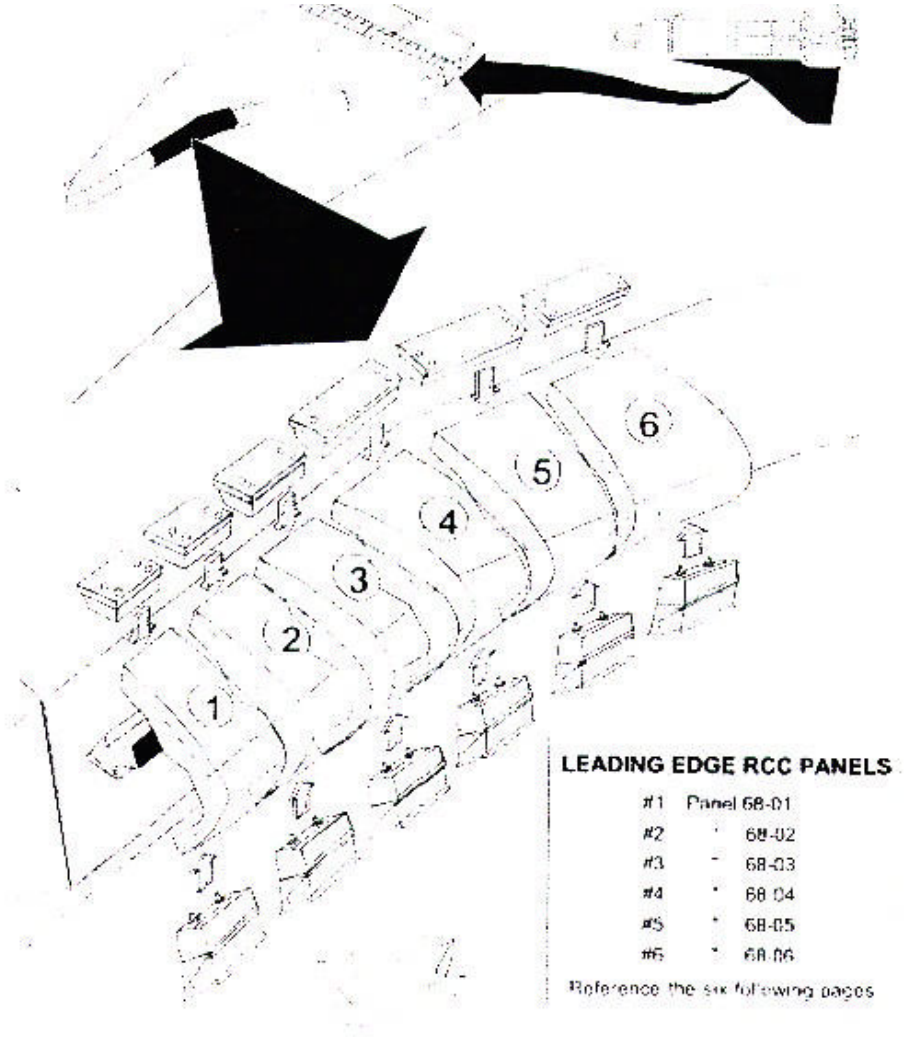

3/14/03

Figure 5

RCC Panel 9 Sensor Locations

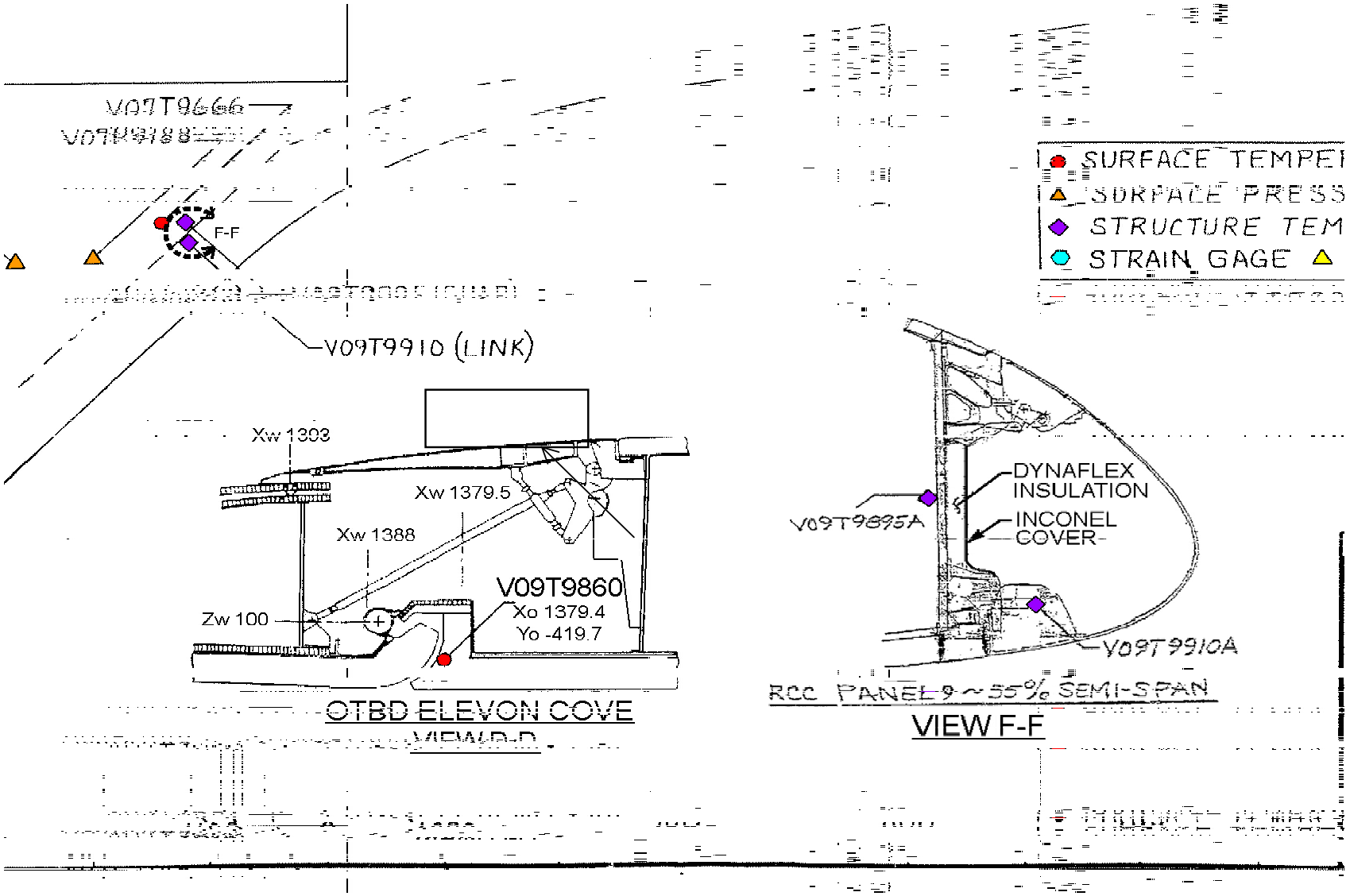

CA-000112

Figure 6

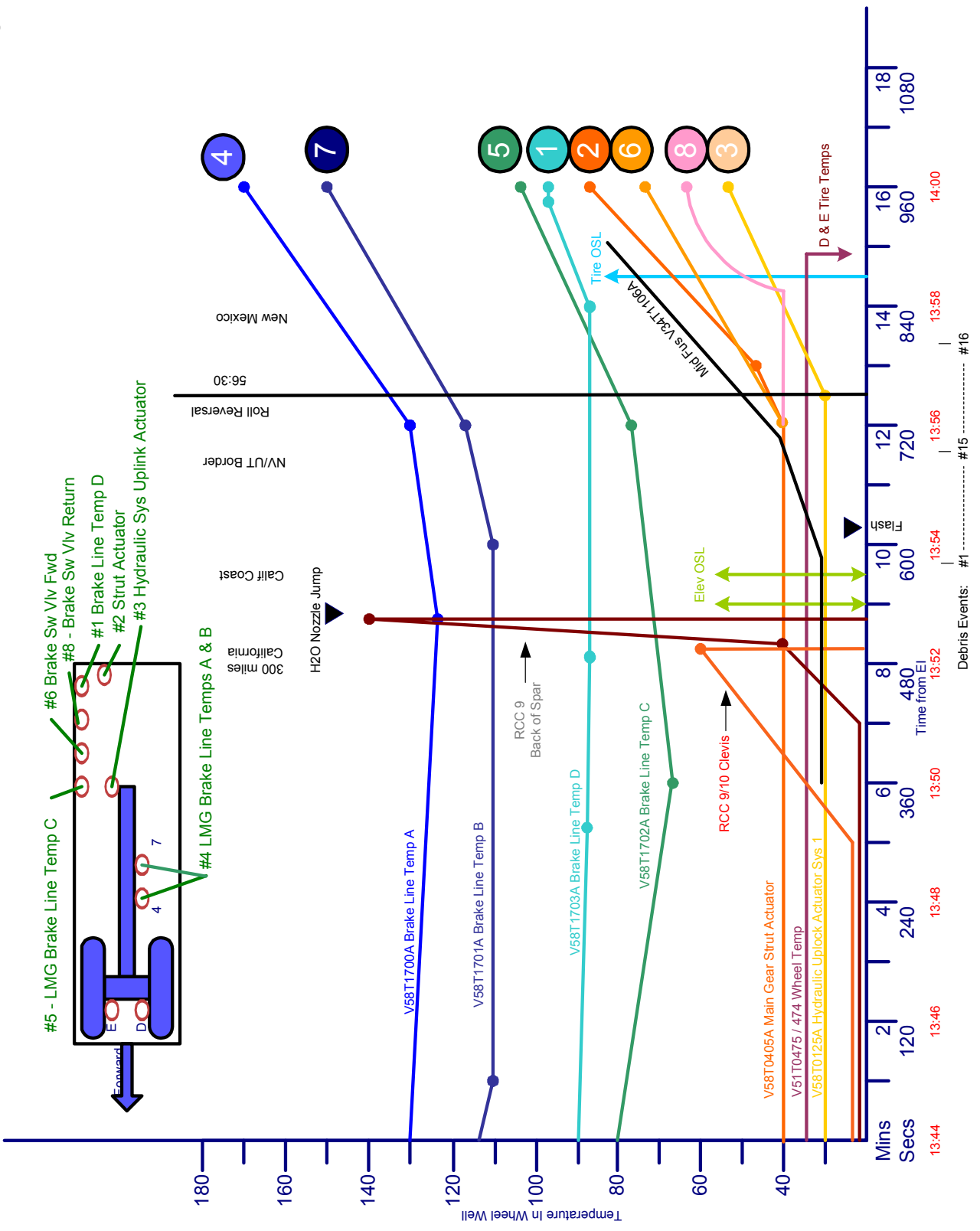

CA-000112

2 Fatal Reentry of STS107 Data and Observations.ppt

CAB068-0209

Figure 7

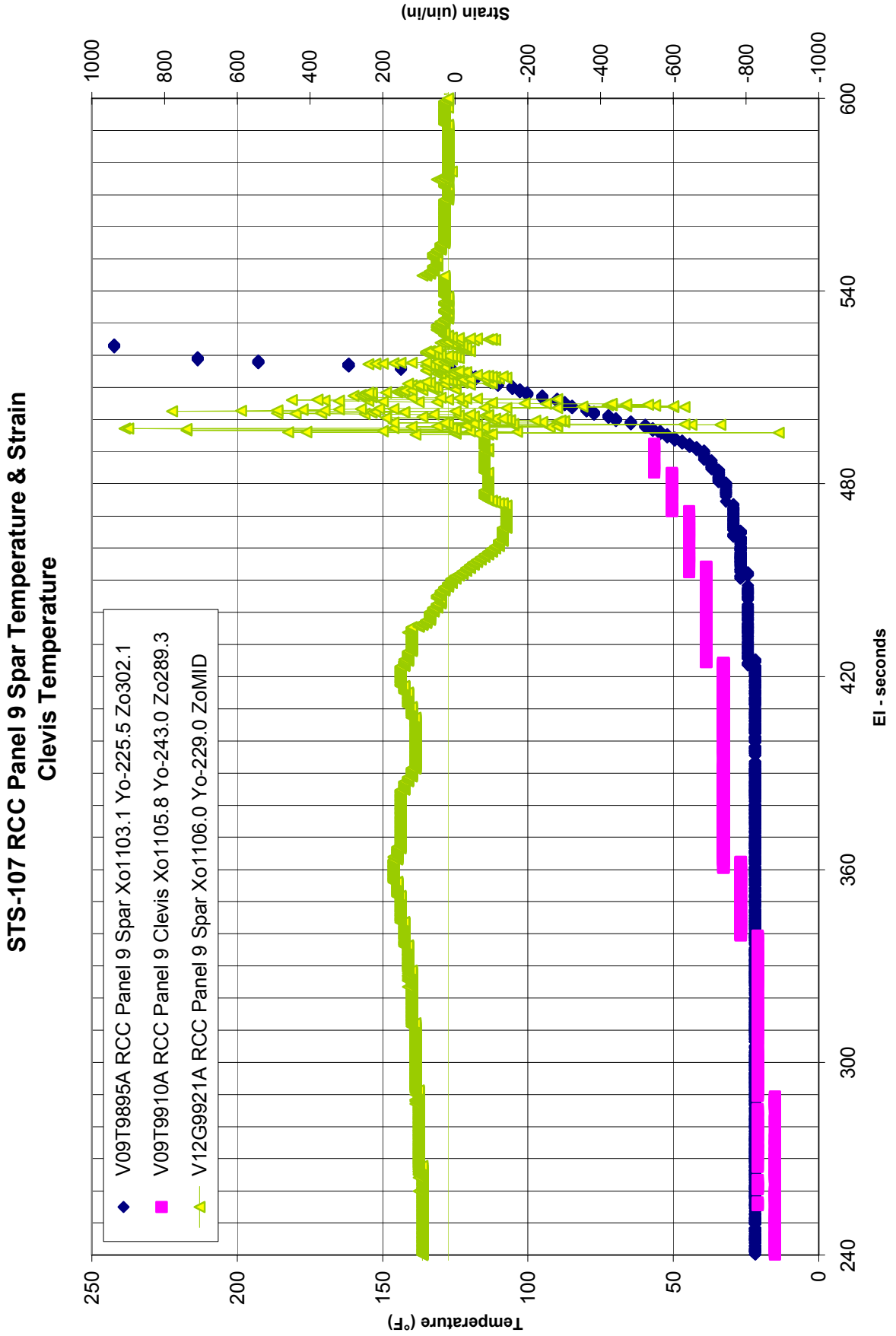

CAB068-0210

CA-000112

2 Fatal Reentry of STS107 Data and Observations.ppt

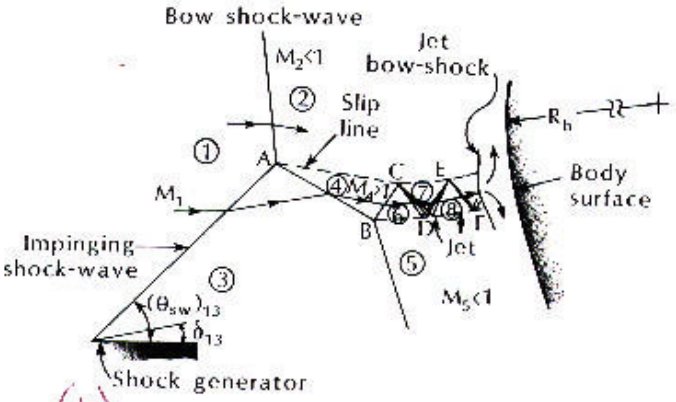

(b)

Fig. 9.14 Type IV shock/shock interaction pattern.

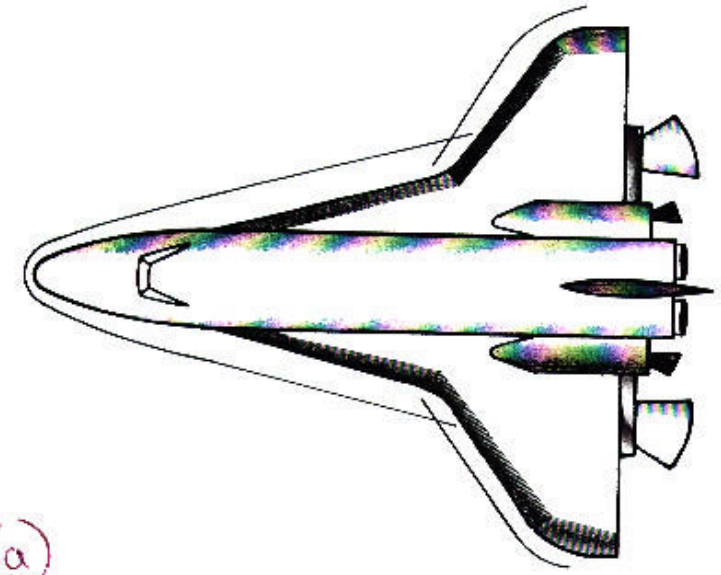

(a)

Fig. 9.3 Interactions between the bow shock wave and the

wing leading edge shock wave

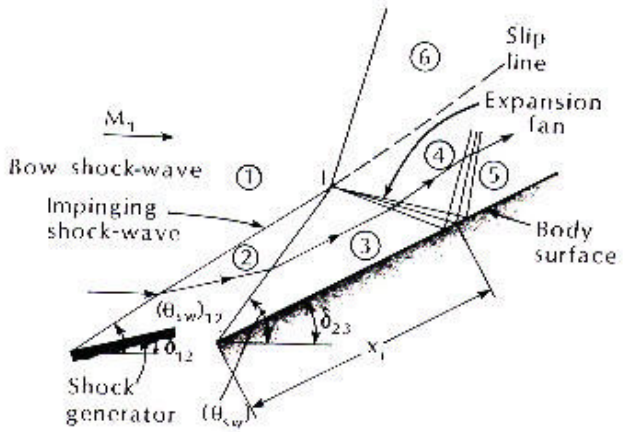

Fig. 9.19 Type VI shock/shock interaction pattern.

(c)

Surface Temperatures Radiation Equilibrium

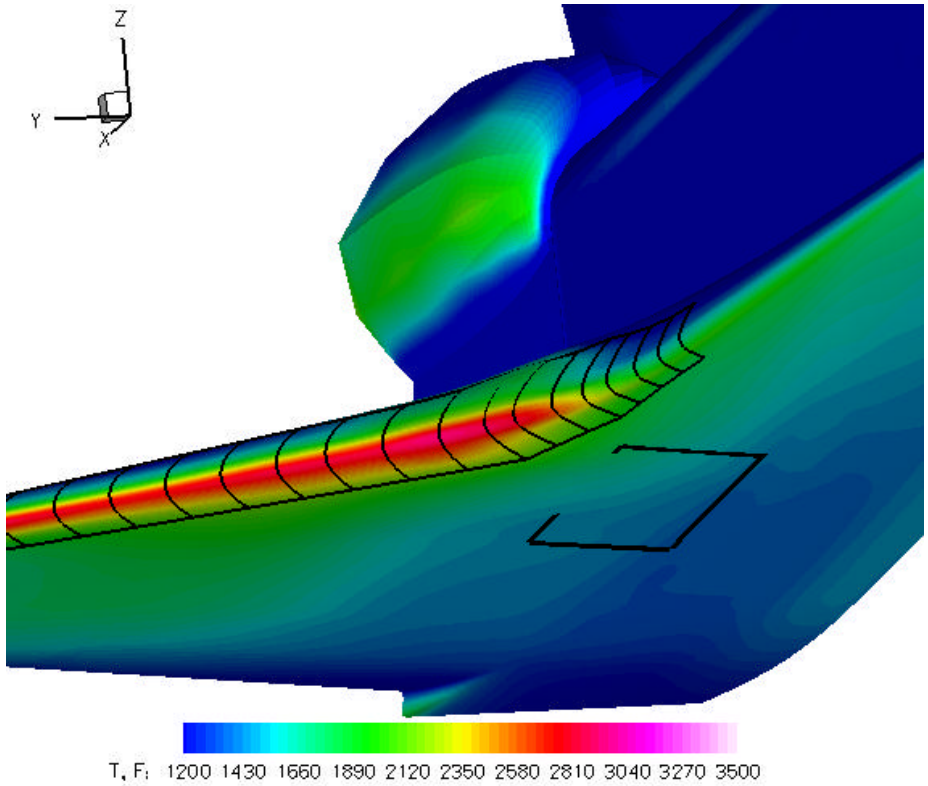

Temperatures, F

CFD Point #1

NASA LaRC LAURA CFD Solution

CFD Point #6

NASA ARC GASP CFD Solution

Temperatures, F

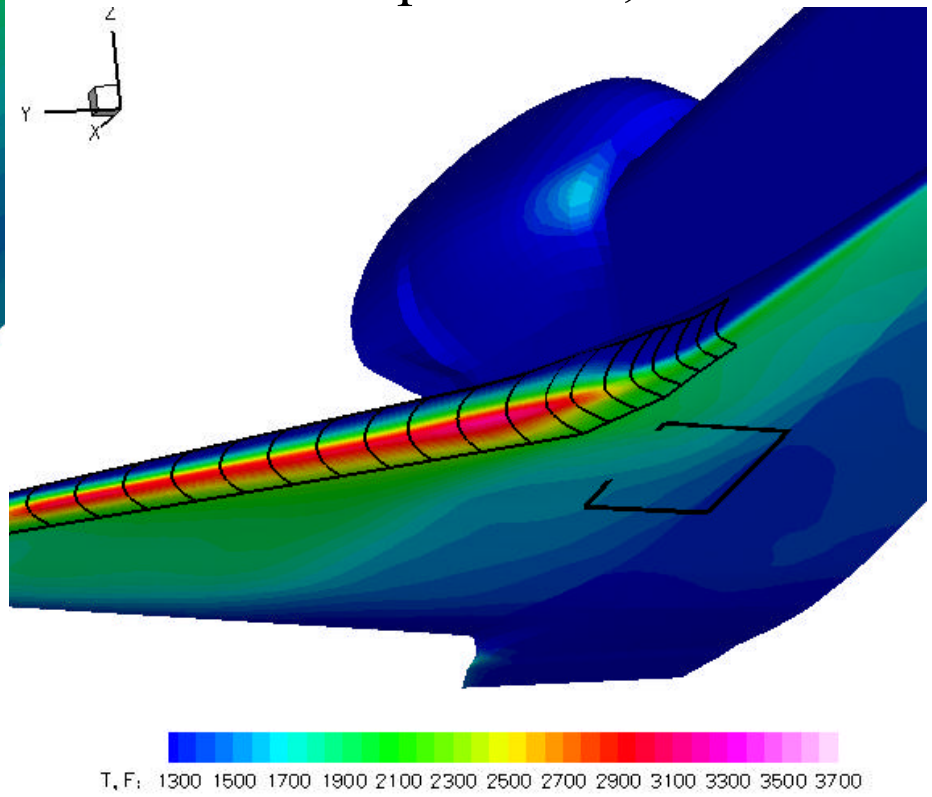

CA-000112

Hot gases enter the chunnel

- Flow behind RCC
- Outward through Chunnel

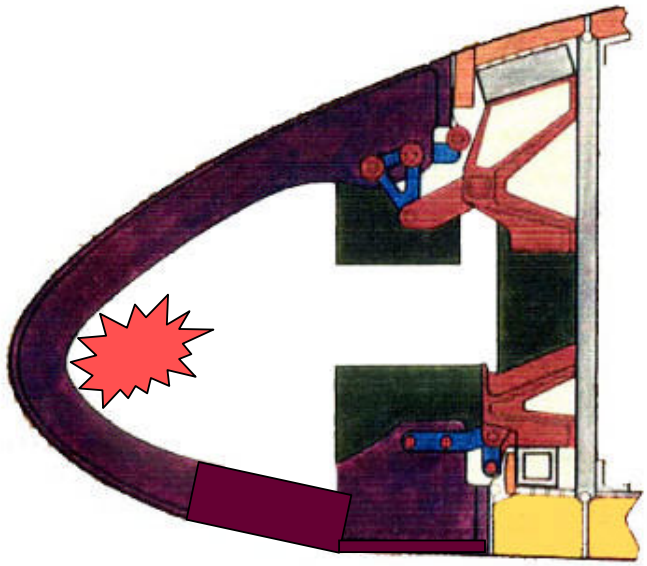

Jet of hot gases coming down the chunnel

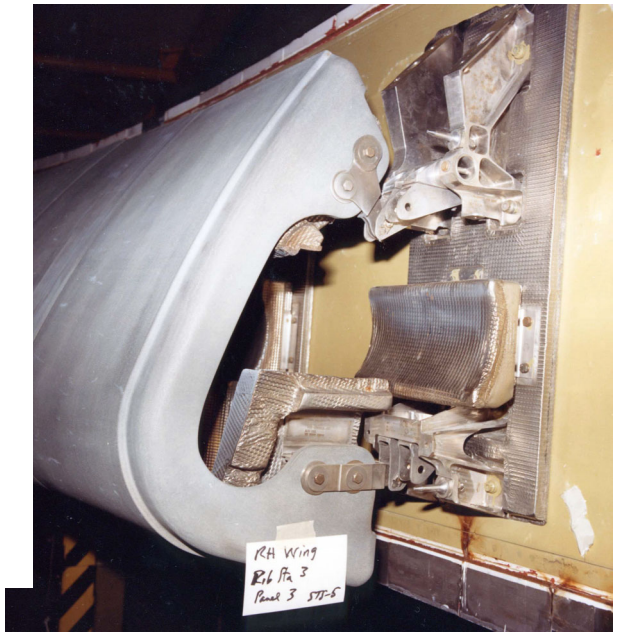

RCC
Aluminum
LI2200
LI900
Inconel-Dynaflex
Inconel 718
A-286 steel

Figure 11

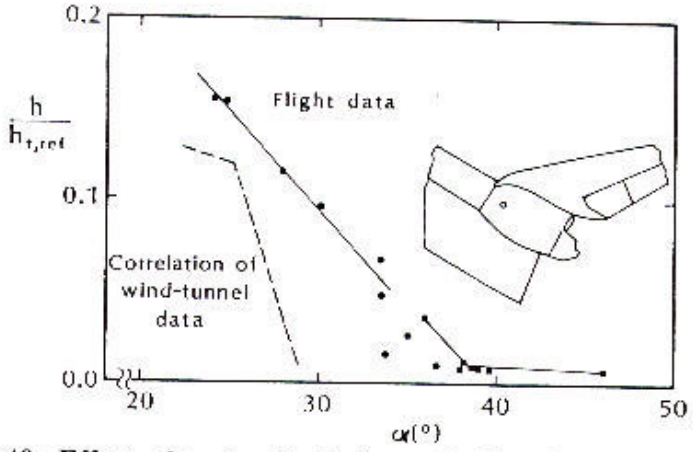

Fig. 9.40 Effect of angle-of-attack on the heating to the OMS pod, as taken from Ref. 38.

Orbiter OML Sensitivity CFD Analysis

Orbiter with RCC Panel 6 Removed – Mach 23.8

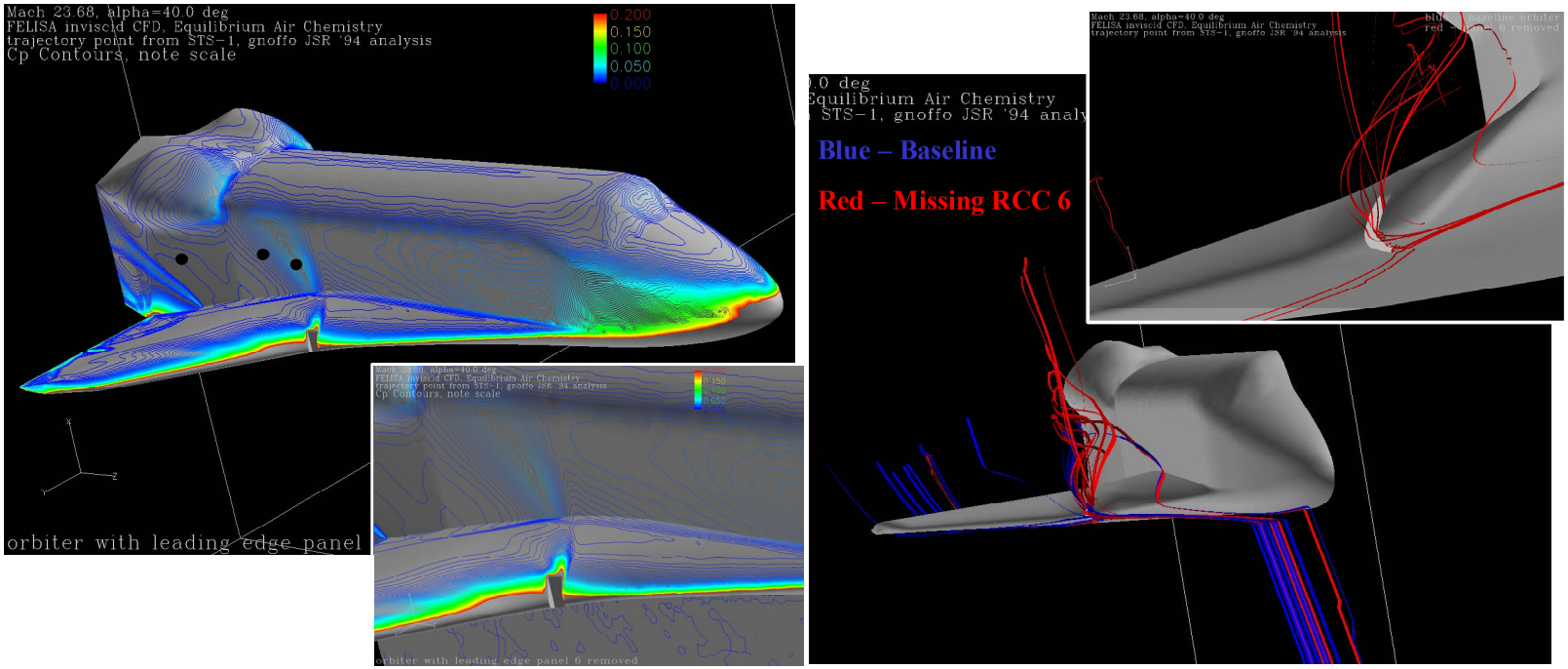

Results and Observations (CFD analysis)

- Produces negative roll and yaw moments w/small magnitude
- Streamlines for damaged vehicle track inboard of baseline
- Resultant shock raises pressure in proximity to temp measurements

17

Rev. 4 – Preliminary
Limited Distribution
DO NOT FORWARD

Limited Distribution
DO NOT FORWARD

Figure 13

VDM Team

Based on Master Time Line (MTL) 13

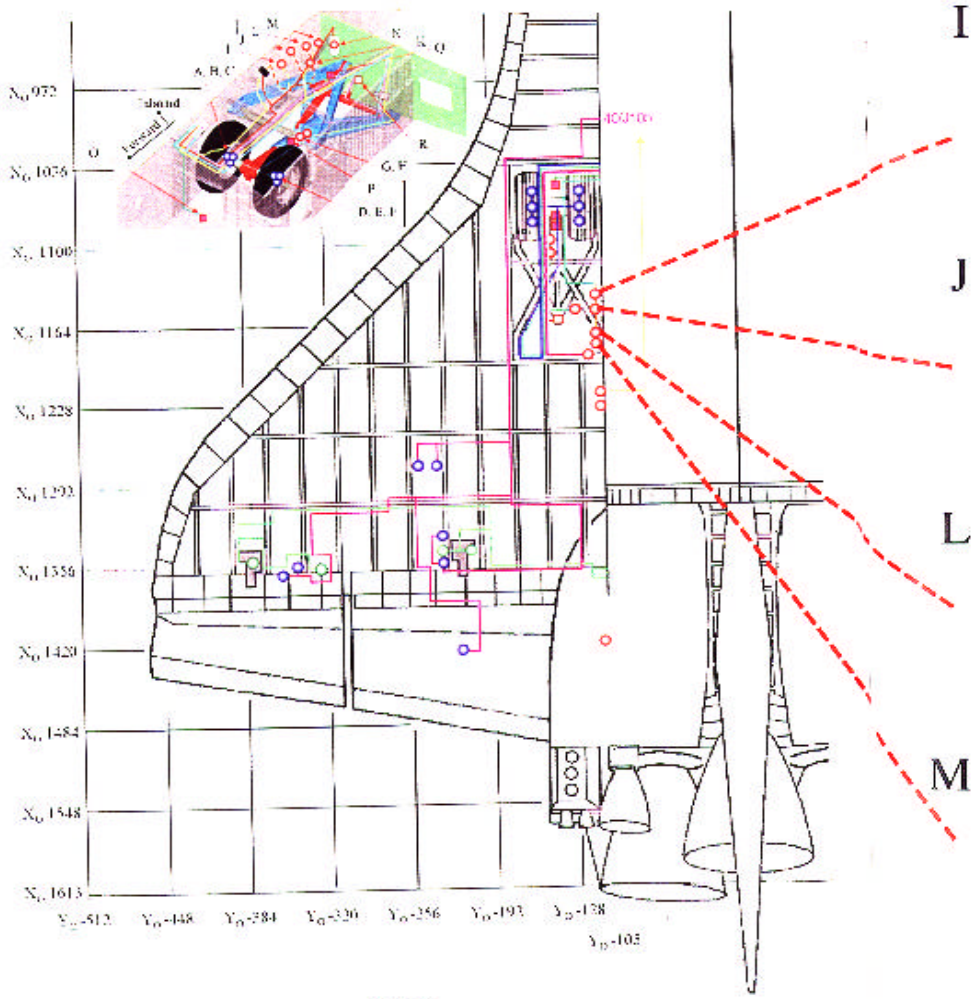

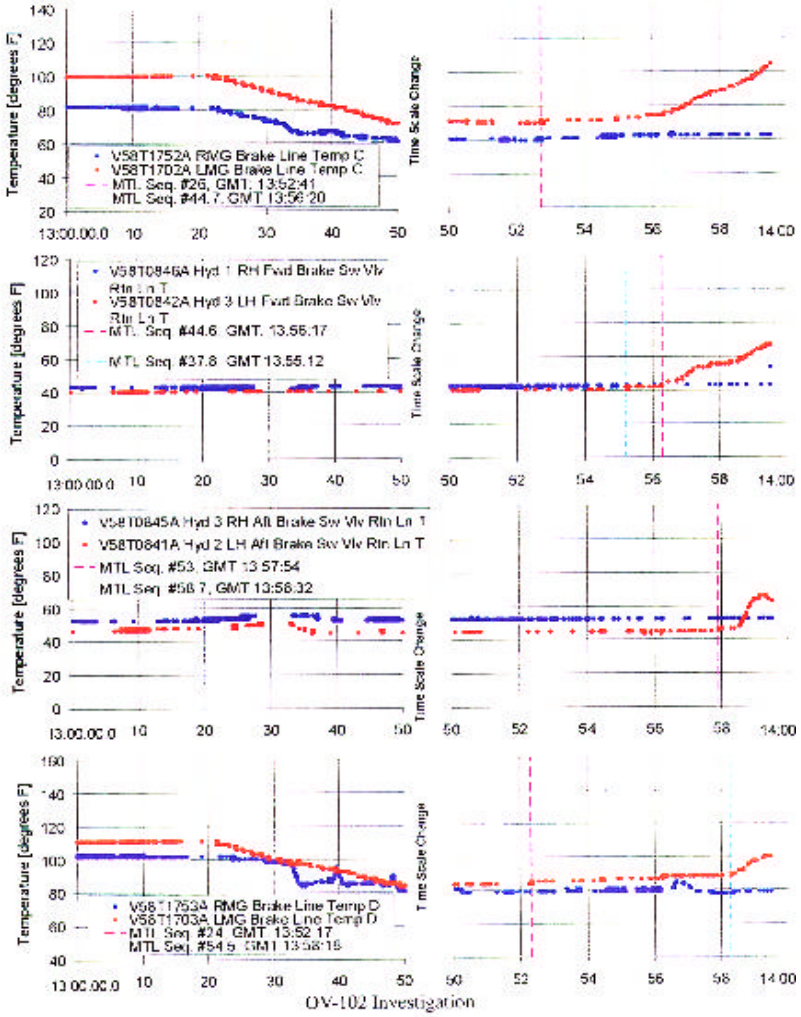

CA-000112

2 Fatal Reentry of STS107 Data and Observations.ppt

CAB068-0216

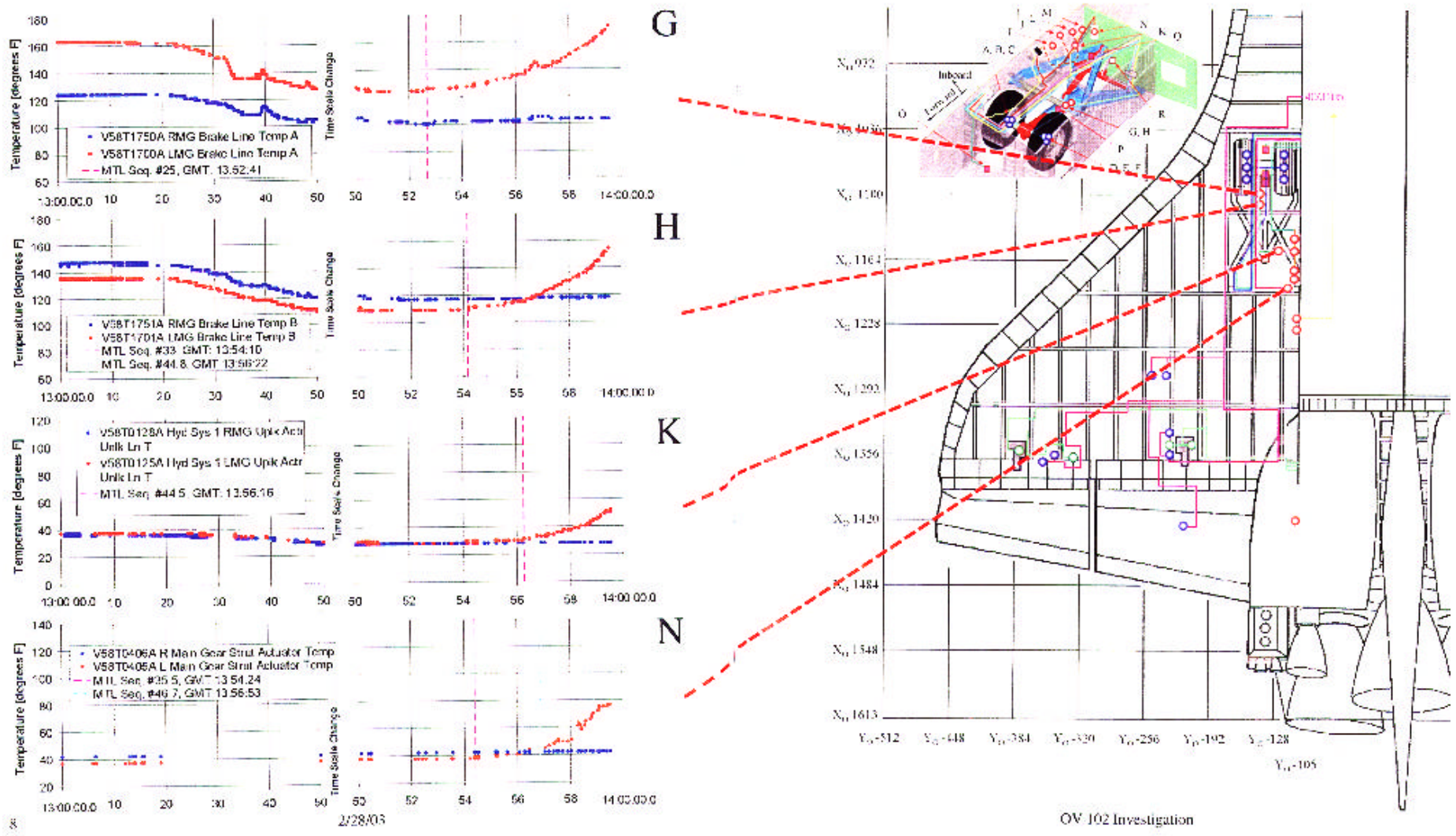
G
H
K
N
Temperature [degrees F]
Time Scale Change
V58T1750A RMG Brake Line Temp A
V58T1700A LMG Brake Line Temp A
MTL Seq. #25, GMT: 13:52:41
V58T1751A RMG Brake Line Temp B
V58T1701A LMG Brake Line Temp B
MTL Seq. #33, GMT: 13:54:10
MTL Seq. #44.8, GMT: 13:56:22
V58T0128A Hyd Sys 1 RMG Upik Actr Unlk Ln T
V58T0125A Hyd Sys 1 LMG Upik Actr Unlk Ln T
MTL Seq. #44.5, GMT: 13:56:16
V58T0406A R Main Gear Strut Actuator Temp
V58T0405A L Main Gear Strut Actuator Temp
MTL Seq. #35.5, GMT: 13:54:24
MTL Seq. #46.7, GMT: 13:56:53
2/28/03
OV-102 Investigation

Figure 15

Wind Tunnel Testing of Orbiter OML Deltas

Effect of RCC Panel Cutout Position on Orbiter Fuselage Nondimensional Heating, Panel 6 vs. Panel 9

Side fuselage heating 2 to 10 times nominal configuration heating.

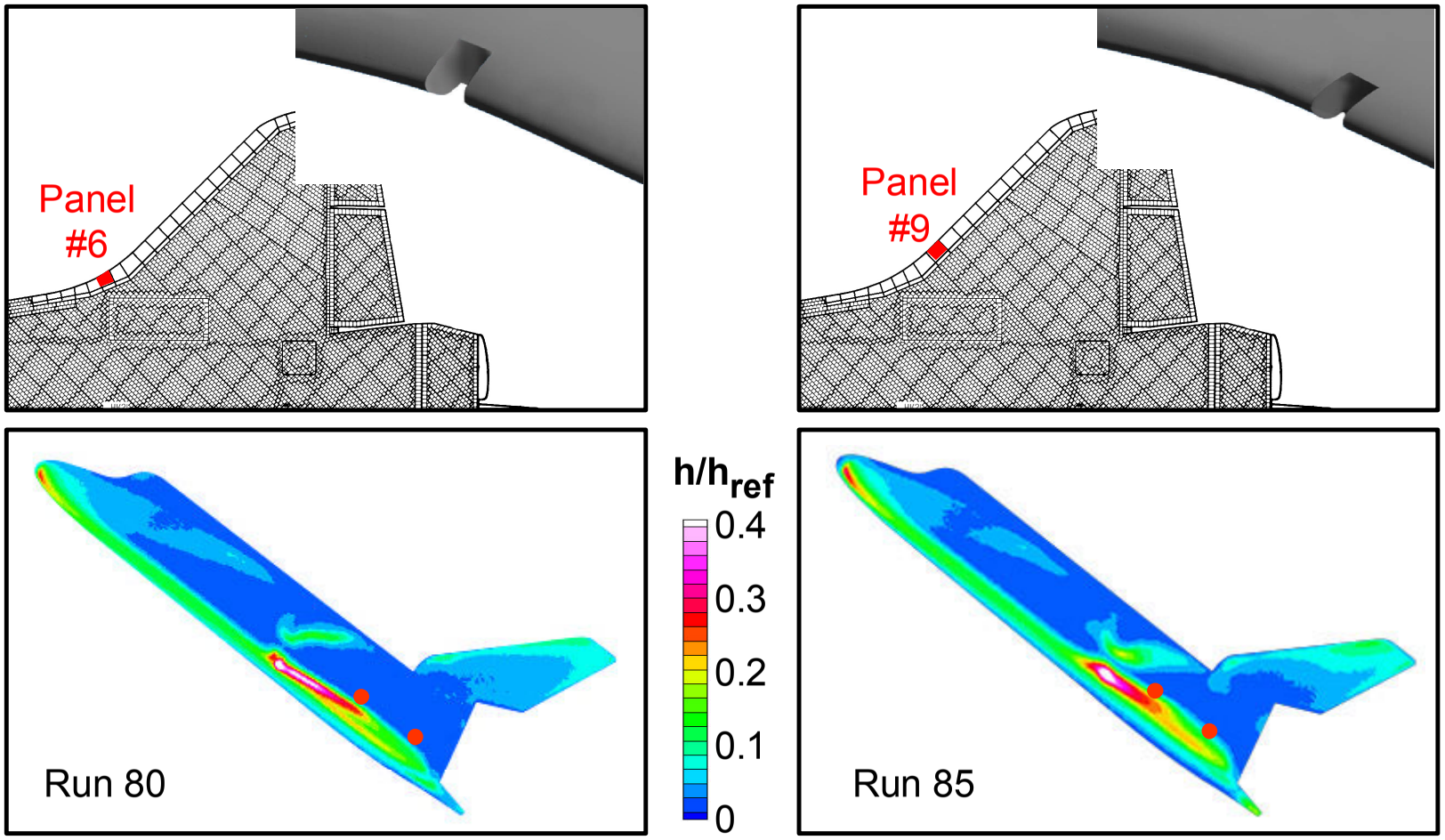

CA-000112

2 Fatal Reentry of STS107 Data and Observations.ppt

CAB068-0218

MADDS Wires on Back of Spar RCC 9 and 8

Figure 16

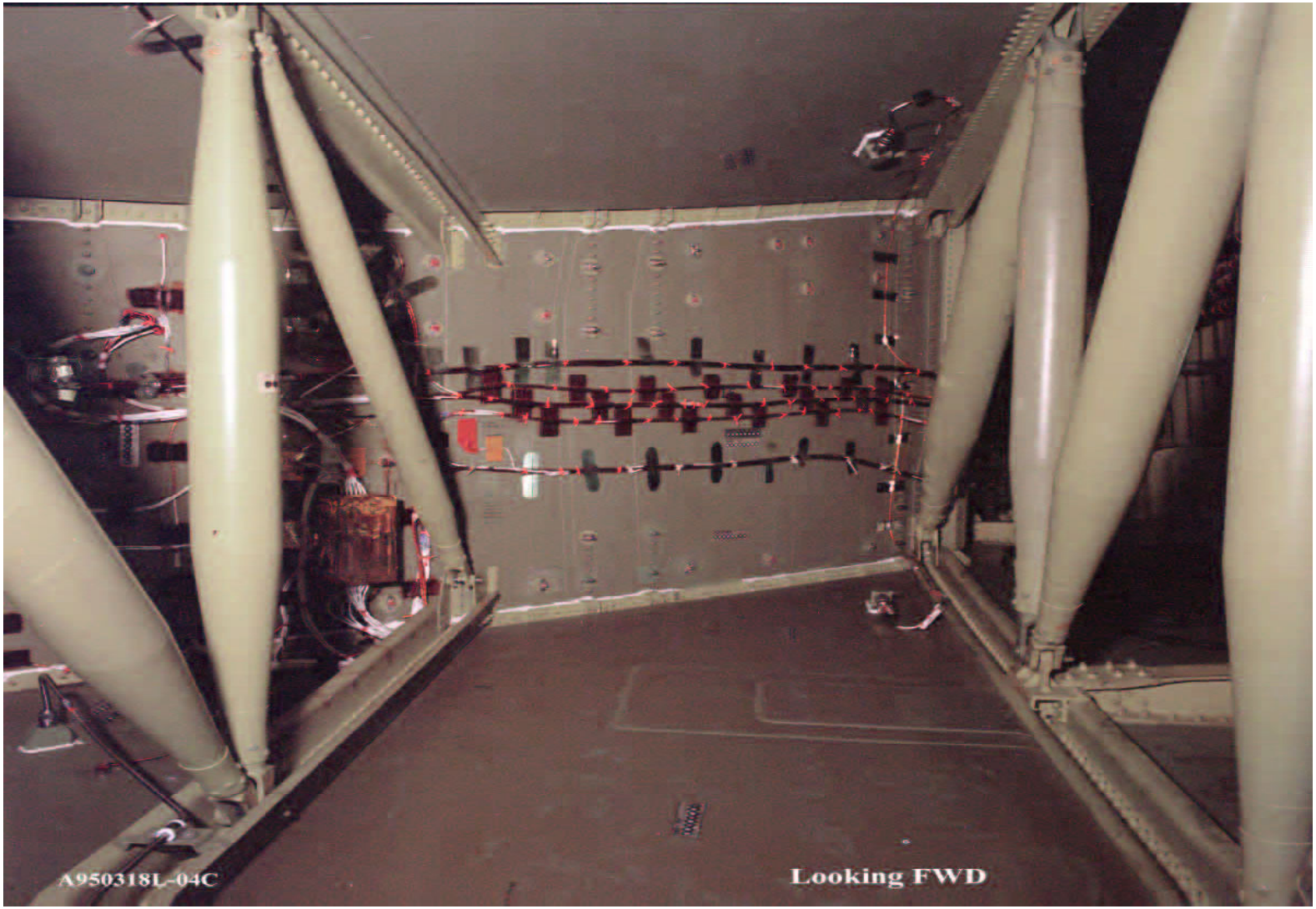

CA-000112

2 Fatal Reentry of STS107 Data and Observations.ppt

CAB068-0219

MADDS Wires on Back of Spar RCC 7 and 6 and IO Wires on Wheel Well

Figure 17

CA-000112

2 Fatal Reentry of STS107 Data and Observations.ppt

CAB068-0220

RCC Spar 5 on MADDS and OI Wires on Front of Wheel Well

CA-000112

2 Fatal Reentry of STS107 Data and Observations.ppt

CAB068-0221

Limited Distribution
DO NOT FORWARD

Figure 19

CA-000112

2 Fatal Reentry of STS107 Data and Observations.ppt

CAB068-0222

Figure 21

Relative Metallic Deposition on Left Wing Materials

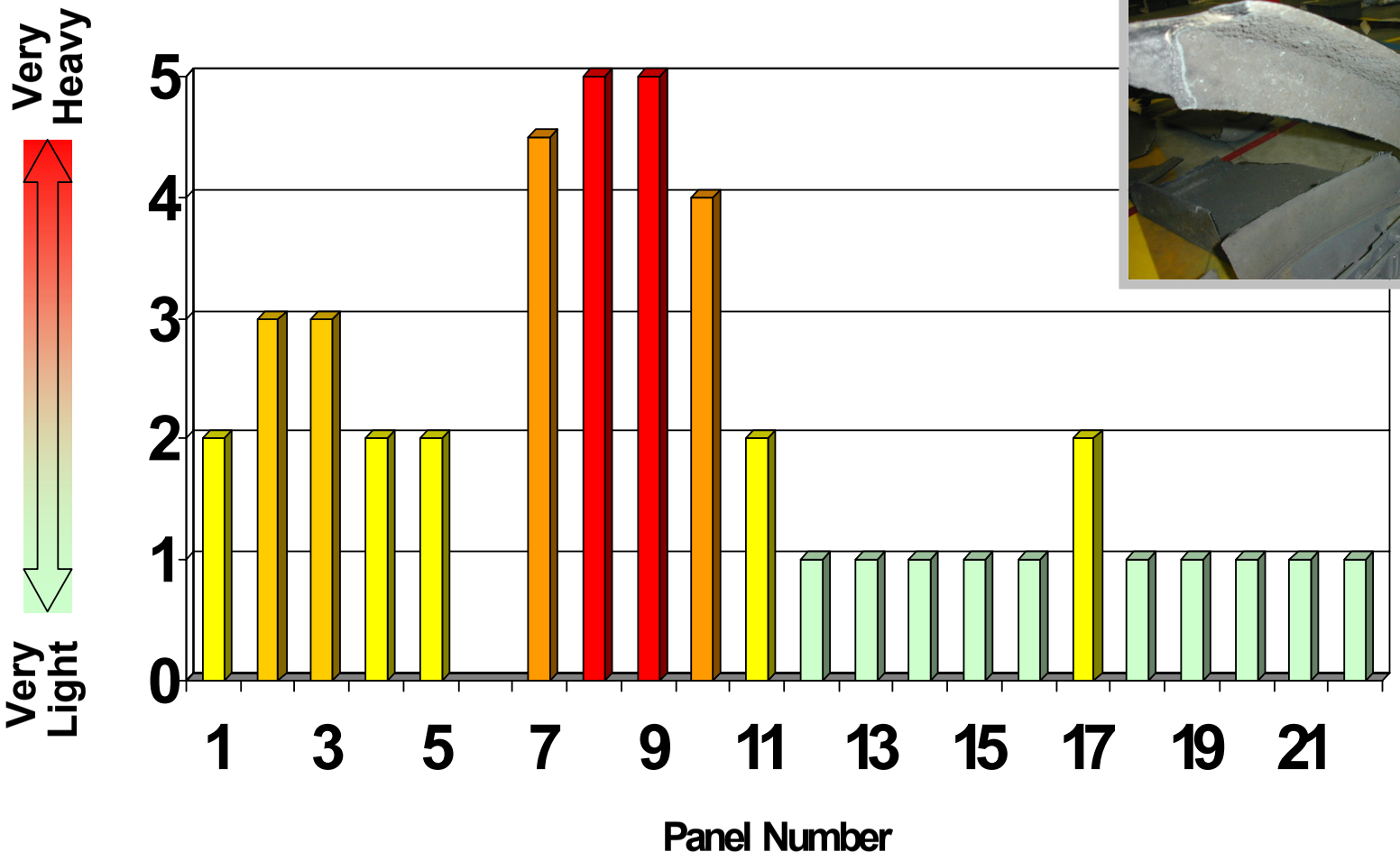

Distribution of metallic deposition volume was centered around panels 8 & 9

CA-000112

View From Bottom of Left-Wing (Similar to Kirtland Photography)

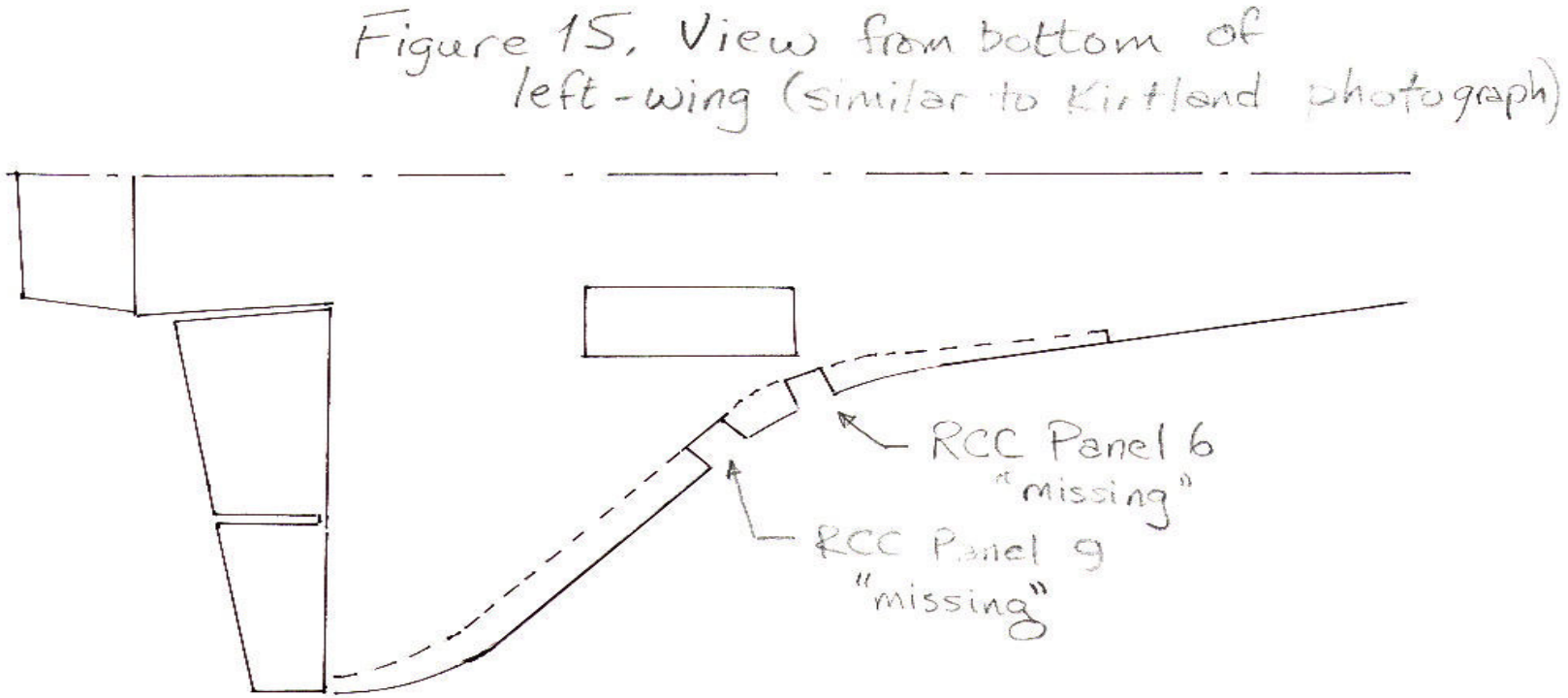

Figure 23

Shock-Shock Interaction for Left Wing, as Modified by Missing RCC Panels (RCC Panel 6 and RCC Panel 9)

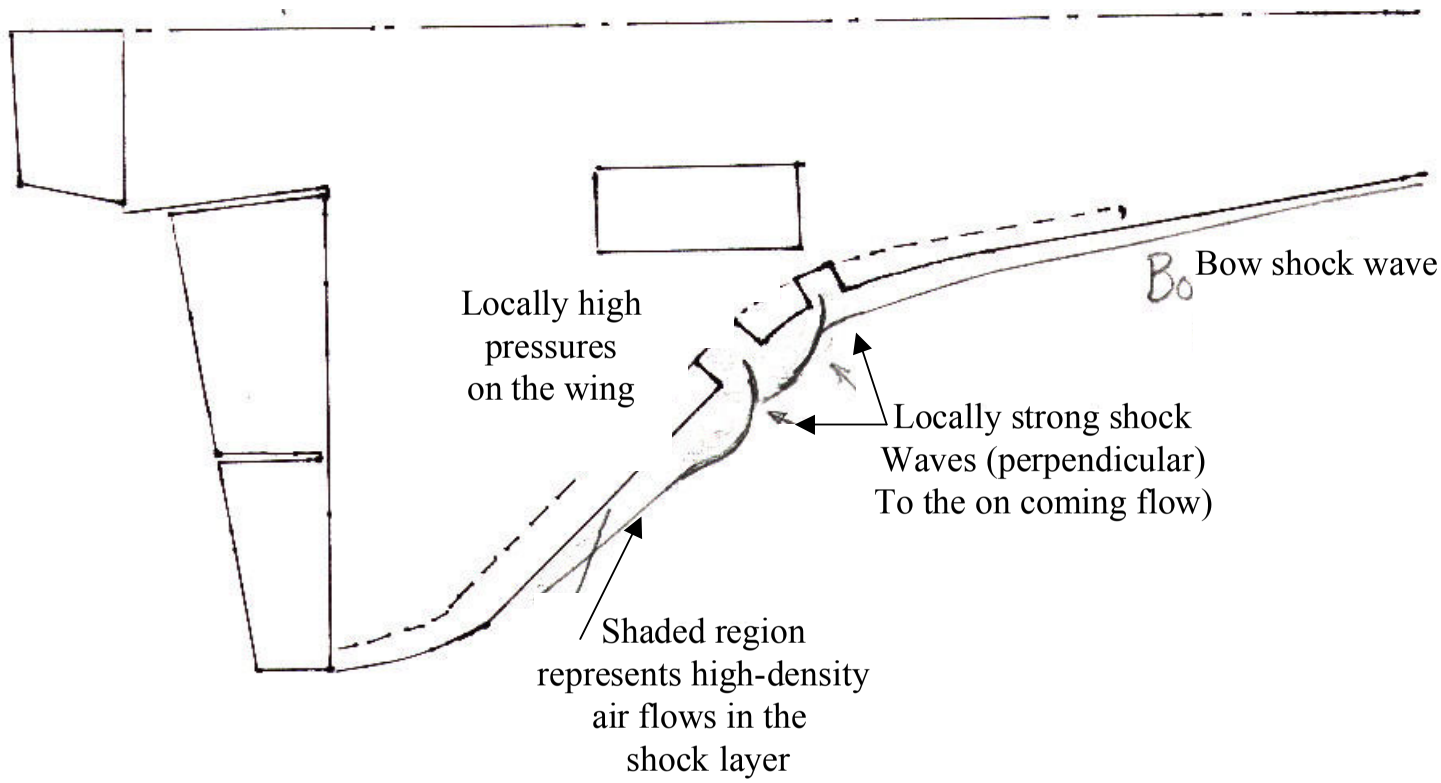

Orbiter Leeside Heating and Corresponding Shock Pattern

Mach 6 Air $\gamma_{eff} = 1.4$ $\alpha = 40$ deg $Re_{\infty, L} = 2.4 \times 10^6$ $\beta = 0$ deg

Note scale change

OMS pod heating increase

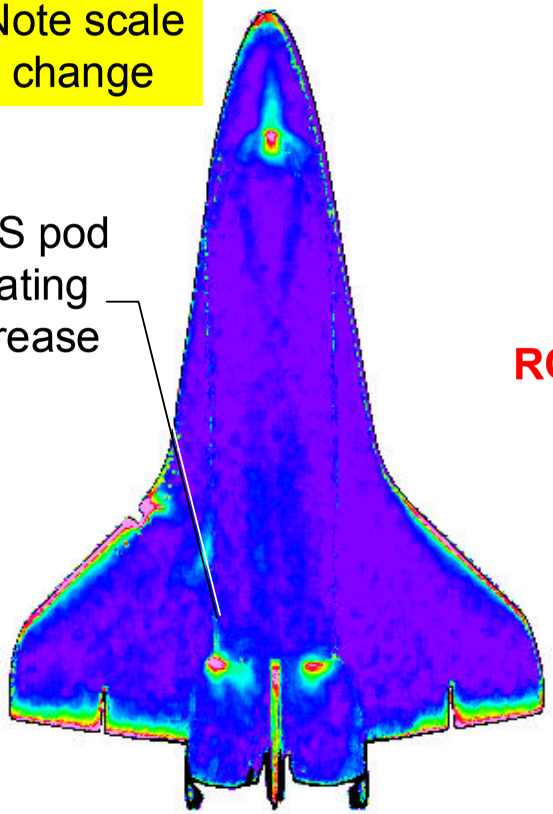

Missing RCC panel #9

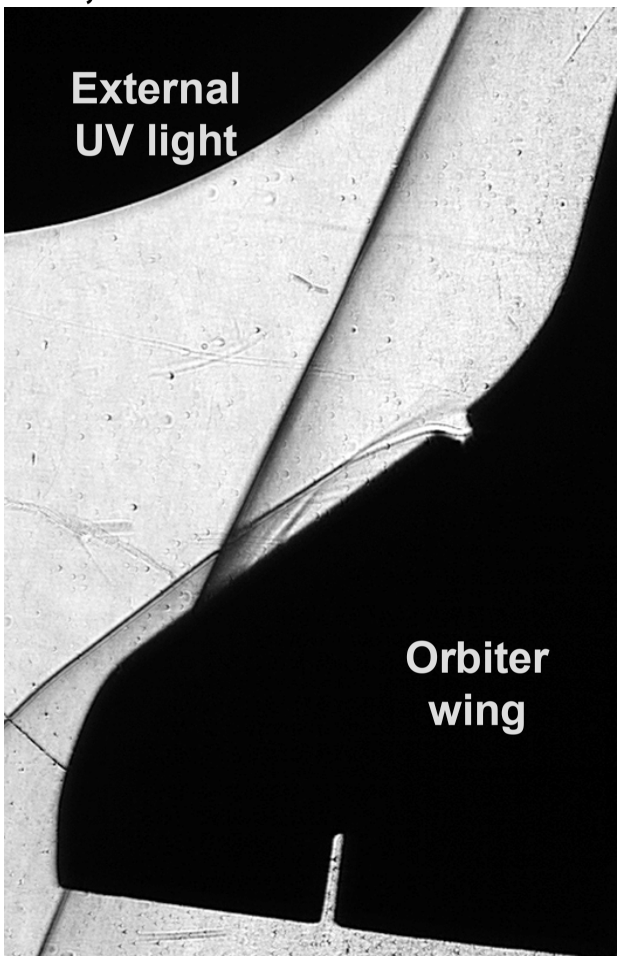

Leeside heating pattern

Shock patterns (path integrated)

CA-000112

2 Fatal Reentry of STS107 Data and Observations.ppt

CAB068-0229

Figure 25

Kirtland Image

Image straight overhead from Albuquerque
Approximately 13:57:24 GMT

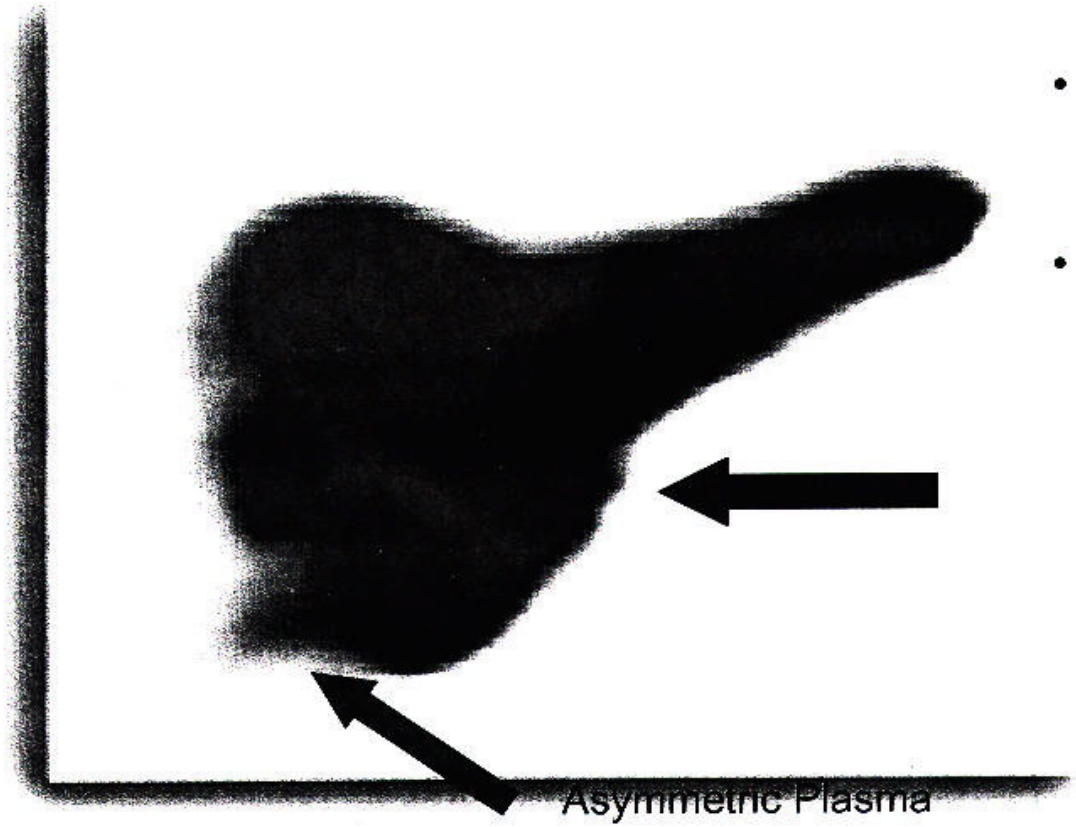

- Gregg Byrne's team thinks this apparent feature is real
- **Are RCC panels hinged up?**

Predecisional Working Draft

CA-000112

Kirtland Image

Image straight overhead from Albuquerque
Approximately 13:57:24 GMT

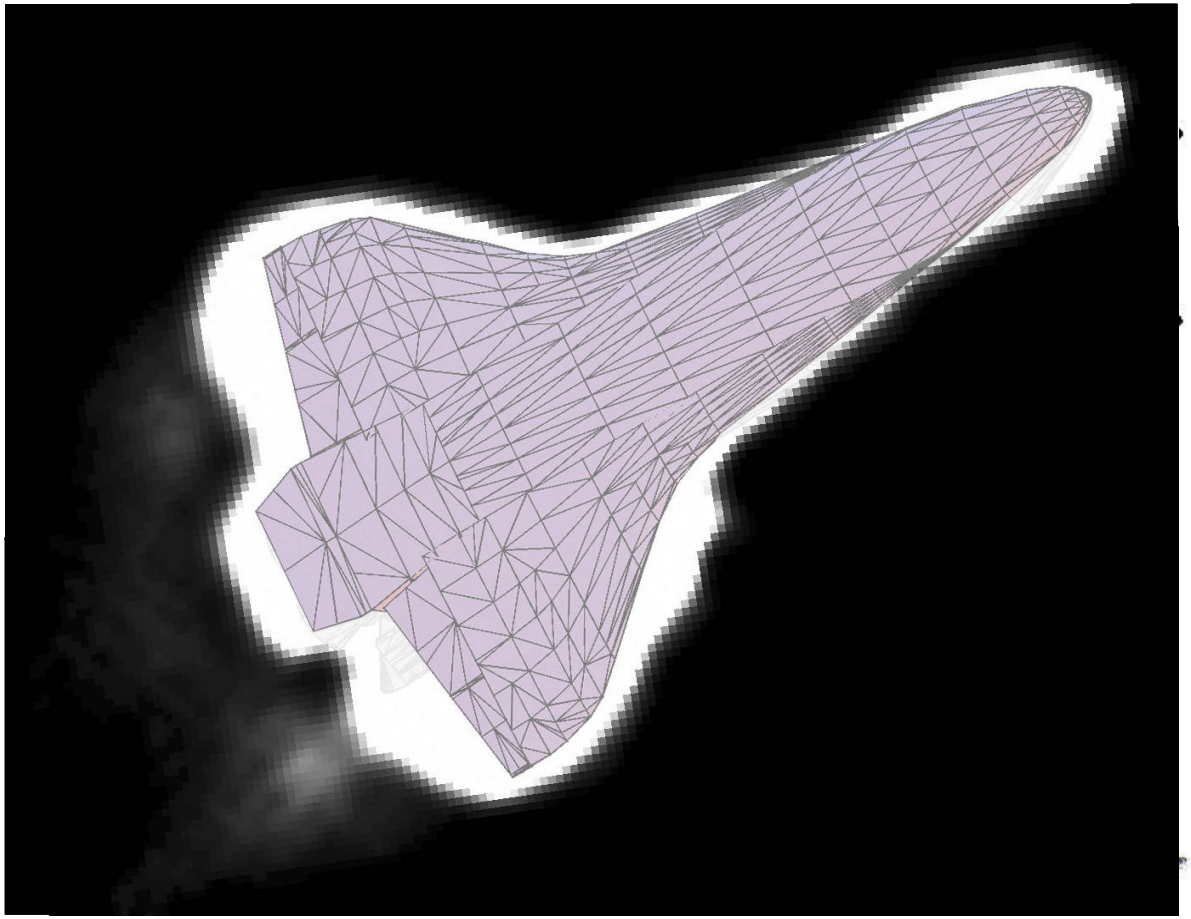

Gregg Byrne's team thinks this apparent feature is real

Are RCC panels hinged up?

CA-000112

2 Fatal Reentry of STS107 Data and Observations.ppt

CAB068-0231

Figure 27

Kirtland AFB Photo at 13:57:19

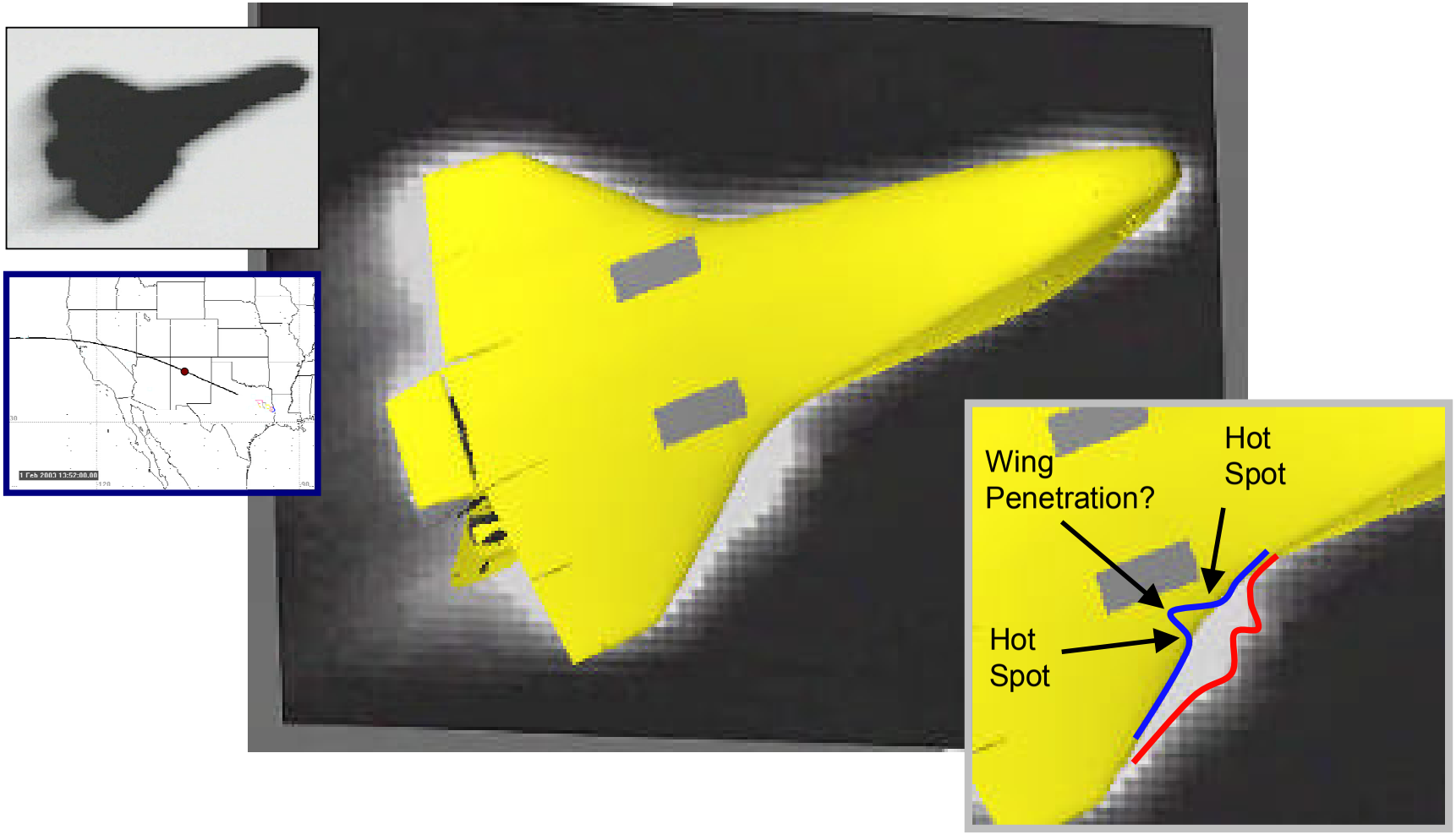

CA-000112

2 Fatal Reentry of STS107 Data and Observations.ppt

CAB068-0232

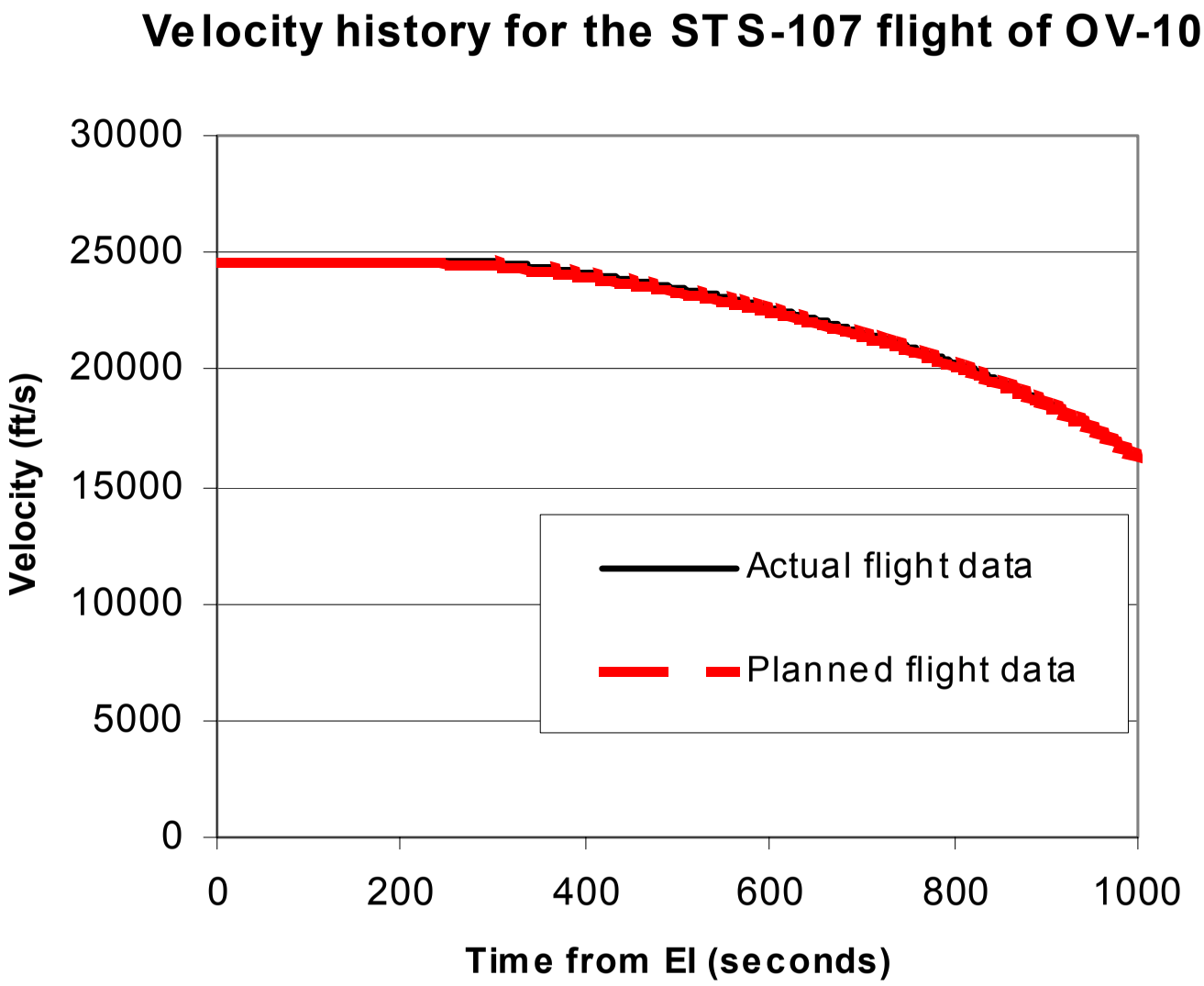
Velocity history for the STS-107 flight of OV-102
Velocity (ft/s)
30000
25000
20000
15000
10000
5000
0
0
200
400
600
800
1000
Time from EI (seconds)
Actual flight data
Planned flight data

Figure 29

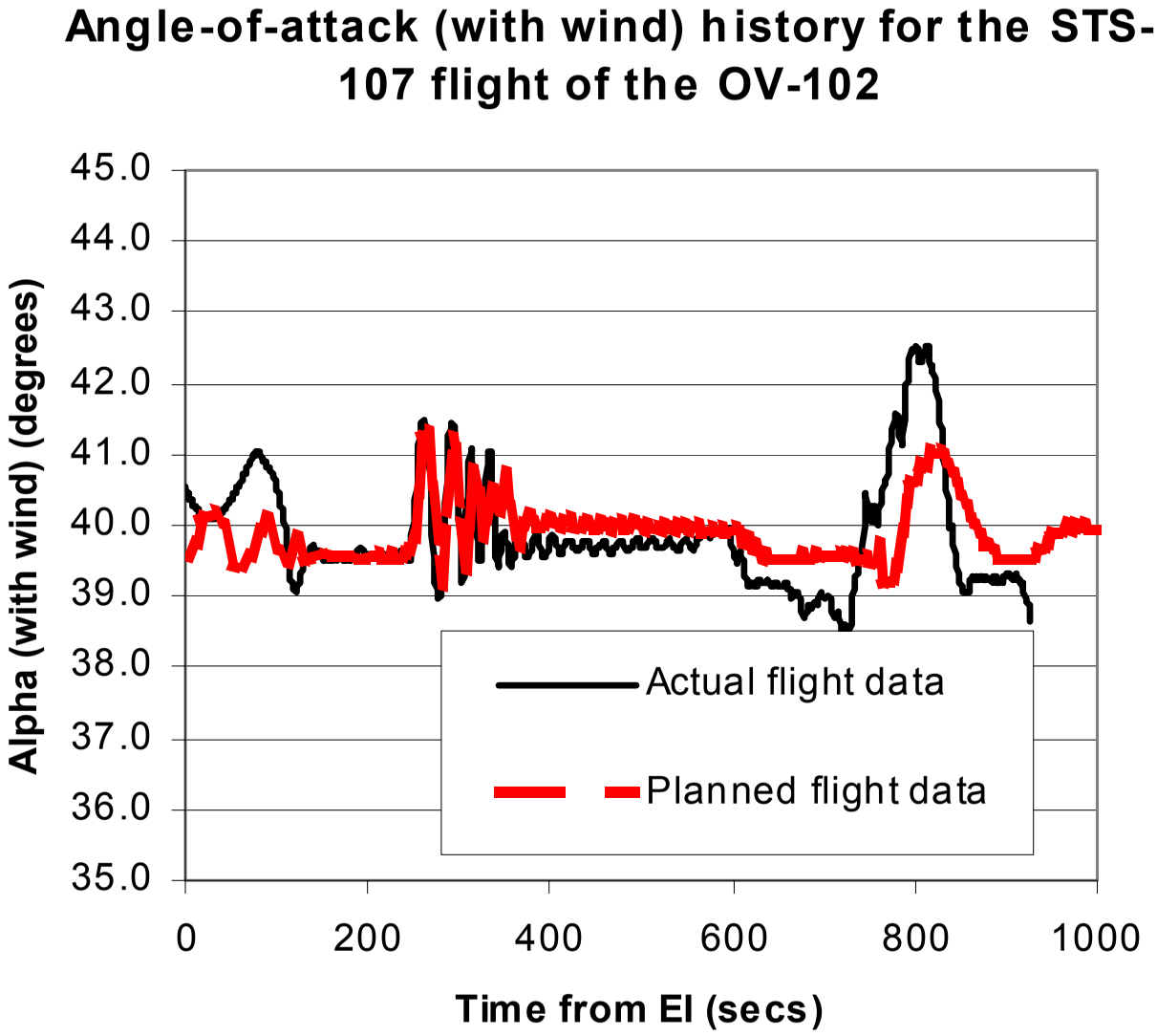

CA-000112

2 Fatal Reentry of STS107 Data and Observations.ppt

CAB068-0234

Sharp Change in Rolling Moment

Timeline Events vs. Δ Roll Aero Model Key Correlations

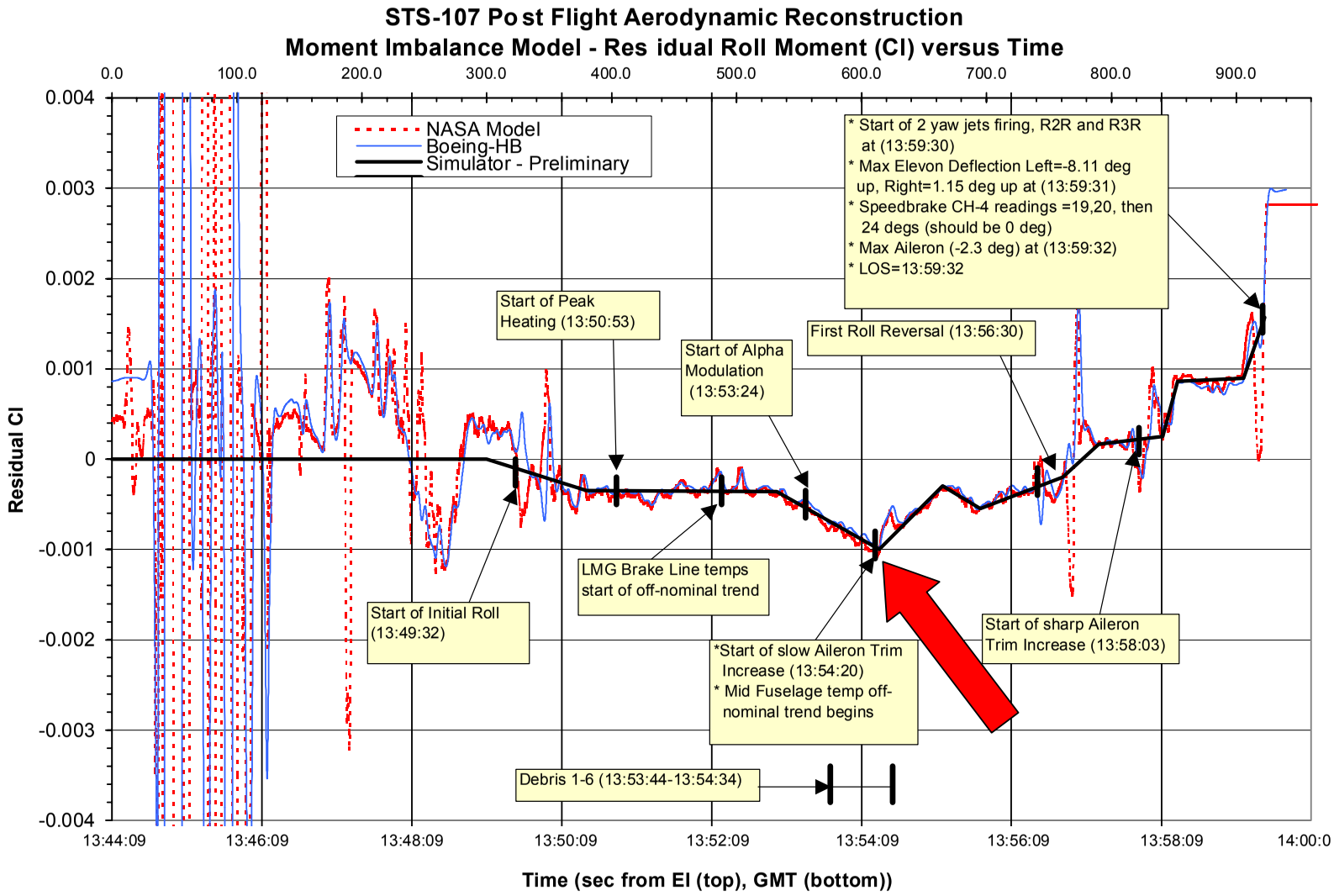

CA-000112

2 Fatal Reentry of STS107 Data and Observations.ppt

CAB068-0235

Figure 31

Missing RCC Panel 9 – Surface Flow Features

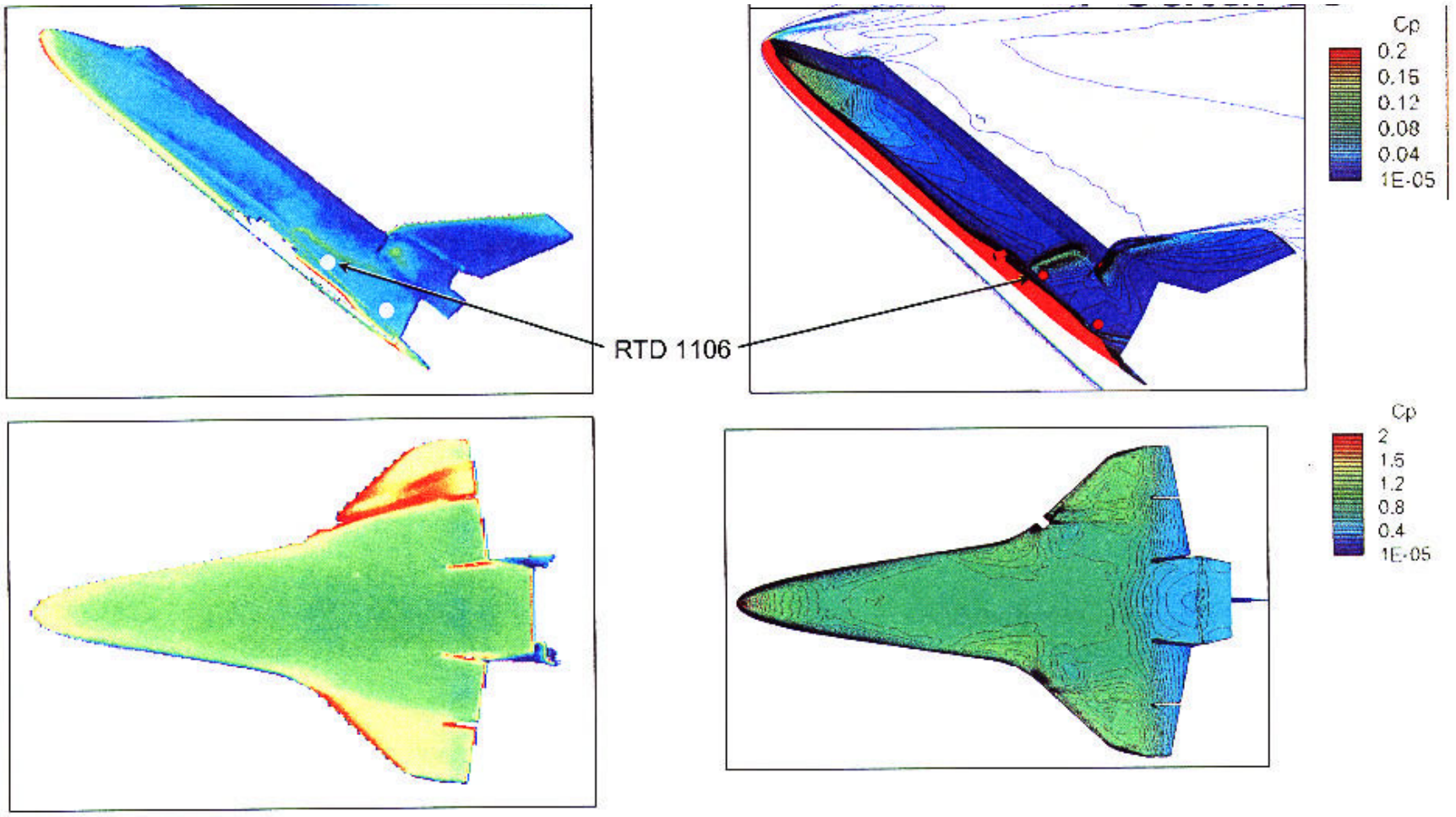

Experimental Aeroheating
20-inch CF4 tunnel, $\alpha = 40°$

FELISA Prediction of Surface Pressure
M = 24.2, Equilibrium air, $\alpha = 40°$

CA-000112

STS-107 Mishap Investigation - Combined Summary Time Line
-BASELINE-

Integ Time Line Team - REV 17 BASELINE **5/8/2003 11 AM**

Note: Rev 17 BASE integrates the OEX data timeline with the Baselined Rev 16 timeline plus IEE aero event changes (accounted for wind effects in aero increment derivation process).
Rev 17 was baselined by the OVE Working Group Team as of 5/7/03.

Sum No.	GMT GMT Day 32	EI sec	OEX data	Milestone	Entry Event	Remarks	MSID
1	13:10:39	EI+2010		TIG-5	APU 2 Start		
2	13:15:30	EI-1719		TIG	OMS TIG		
3	13:18:08	EI-1561			OMS End of Burn		
4	13:31:25	EI-764		EI-13	APU 1 Start		
5	13:31:29	EI-760			APU 3 Start		
5.5	13:39:28.559	EI-280.4	X		Start of OEX PCM Data Block		
6	13:44:09	EI+0		EI	Entry Interface (400,000 ft)	Mach 24.57	
6.1	13:45:39 / 48:59	EI+90 / EI+290	X		16 Temperature Sensors on the lower surface to the left of or at the centerline experience off-nominal early temperature trends (warmer temperature rise rate compared to previous flights of OV-102 at the same inclination)		V09T9849A V07T9784A V07T9666A V07T9786A V07T9468A V07T9787A V07T9470A V07T9788A V07T9711A V07T9478A V07T9713A V07T9480A **V07T9785A V09T9845A V09T9231A V07T9489A**
6.15	13:48:39	EI+270	X		Left Wing Front Spar at RCC Panel 9 - initiation of off-nominal trend in strain (small increase) followed by a more significant off-nominal signature to failure at EI+495 secs	The measurement began to fail at approximately EI+495 sec	V12G9921A X1106.0 Y-229.0 ZMID
6.2	13:48:59	EI+290	X		Left Wing RCC Panel 9 Lower Attach Clevis (between RCC 9 and 10) - initiation of an off-nominal temperature trend (early temperature increase compared to previous flights of same inclination)	The measurement began to fail at approximately EI+492 sec	V09T9910A X1112.0 Y-239.0 Z289.0
6.3	13:49:32	EI+323			Start of initial roll		
6.4	~13:49:39*	~EI+330*	X		Left Wing Front Spar Caps Strain Gage shows early off nominal downward trend	*Note: PCM3 entry data is in snapshot format (not continuous). Time indicated is at start of data segment where off-nominal signature is first observed, therefore event may have started earlier than noted.	V12G9169A X1107 Y232 Z?
6.45	13:49:49 / 49:59	EI+340 / EI+350	X		4 Left OMS Pod Surface temps - Start of off-nominal temperature trend - cooler rise rate when compared to previous flights of same inclination	Followed by the start of a warmer-than-expected temperature trend beginning in the EI+510 to EI+540 sec range	V07T9976A V07T9978A V07T9220A V07T9972A
QBAR = ~15 psf (~0.10 psi); Mach 24.4					**------ 32:13:50:00 ------**	EI + 351 sec; WLE Stagnation Temp: ~2520 F (STS-107 Nom EOM Design Pred)	
6.5	13:50:00 / 43	EI+351 / EI+394			Five events of unexpected return link comm drop-out (Comm events 1-5)	On upper left aft antenna (TDRS 171/W). Appears off-nominal based on previous flt data. Comm loss not continuous thru period indicated.	
6.7	13:50:09	EI+360	X		Left PLBD Surface TC BP3703T - Start of off-nominal temperature trend - cooler rise rate when compared to previous flights of same inclination	Followed by large increase in temperature at EI + 570 seconds	V07T9925A X1138.5 YLH Z441.4
6.9	13:50:19	EI+370	X		Left Wing Lower Surface Thermocouple BP2510T begins off-nominal temp increase from ~2000 deg F to ~2200 deg F over approx 50 seconds followed by a momentary 100 deg F temperature spike	The measurement subsequently fails at approximately EI+496 sec	V07T9666A X1121.1 Y-235.5 ZLWR
7	13:50:53	EI+404		Start of Peak Heating		Determined by analysis	
QBAR = ~19 psf (~0.13 psi); Mach 24.1					**------ 32:13:51:00 ------**	EI + 411 sec; WLE Stagnation Temp: ~2650 F	
7.2	13:51:14	EI+425	X		Left Wing Front Spar at RCC Panel 9 - start of off-nominal increasing temperature trend	Increasing trend continues until the measurement starts to fail at approximately EI+520 sec	V09T9895A X1102.2 Y-239.0 Z-239.0
7.25	13:51:14	EI+425	X		Left Wing RCC Panel 9 Lower Attach Clevis (between RCC 9 and 10) - start of a more rapid off-nominal increasing temperature trend	Increases until the measurement starts to fail at approximately at EI + 492 secs	V09T9910A X1112.0 Y-239.0 Z289.0
7.3	deleted					Rationale for deletion: Upon further evaluation of the data, it was determined that the remote sensor signatures had been seen in previous flights and/or could be explained by known events.	
7.35	deleted					Rationale for deletion: Moved to seq # 11.37 after further analysis.	
7.37	13:51:49	EI+460	X		OMS-L Pod HRS1 Surf T3-AFT - Start of off-nominal higher-than-expected temperature trend when compared to previous flights of same inclination	Sensor sees a sharp temp increase at EI+910 and goes erratic at EI+940	V07T9223A X1437.2 Y-126 Z422
QBAR = ~22 psf (~0.15 psi); Mach 23.7					**------ 32:13:52:00 ------**	EI + 471 sec; WLE Stagnation Temp: ~2700 F	
7.4	deleted					Rationale for deletion: Moved to seq # 8.75 after further analysis.	
7.45	13:52:09 / 52:55	EI+480 / EI+486			Four events of unexpected return link comm drop-out (Comm events 6-9)	On upper left aft antenna (TDRS 171/W). Appears off-nominal based on previous flt data. Comm loss not continuous thru period indicated.	

STS-107 Mishap Investigation - Combined Summary Time Line
-BASELINE-

Integ Time Line Team - REV 17 BASELINE

5/8/2003 11 AM

Note: Rev 17 BASE integrates the OEX data timeline with the Baselined Rev 16 timeline plus IEE aero event changes (accounted for wind effects in aero increment derivation process).
Rev 17 was baselined by the OVE Working Group Team as of 5/7/03.

Sum No.	GMT GMT Day 32	EI sec	OEX data	Milestone	Entry Event	Remarks	MSID	
7.46	13:52:09 / 52:49	EI+480 / EI+520	X		Nose Cap RCC Attach OutBoard Clevis (Chin Panel) - Temporary change in slope, then returns to "nominal" Note: Adjacent sensor V09T9888 (on centerline) does not show this signature		V09T9889A X262.0 Y-23.0 LWR	
7.47	13:52:16	EI+487	X		Two Left Wing and 1 Right Wing Surface Pressure measurements show signs of failure	First OEX data to show signs of failure	V07P8038A V07P8086A V07P8151A	
7.48	13:52:16 / 53:17	EI+487 / EI+522	X		All of the measurements running in the wire bundle along the left wing leading edge show signs of failure		15 of 15 measure-ments	
7.49	13:52:16 / 56:24	EI+487 / EI+735	X		The vast majority of left wing OEX measurements show signs of failure during this time period - this includes all left wing temperature and pressure measurements and all strain measurements aft of Xo 1040 with the exception of three strain measurements on the upper surface of the LMLG compartment Additionally, 30 right wing pressure measurements show signs of failure		Multiple measurements	
7.5	13:52:17	EI+488		Approx Vehicle Ground Location: 39.0 N / -129.2 W	Altitude 236,800 ft / Mach 23.6 - Over the Pacific Ocean, approx 300 miles West of California Coastline	Approx vehicle position when first off-nominal data was seen; Data source: STS-107 GPS Trajectory Data		
7.7	13:52:17	EI+488			LMG Brake Line Temps (D) - small increase in temperature ("bit flip up")	Initiation of temp rise ("bit flip up") - may be nominal based on rise rate comparison w/ flight experience	V58T1703A	
7.75	13:52:18	EI+489	X		Left Wing Spar Cap Lwr L103 (Xo 1040 Spar - Lower Cap) - off-nominal increase in strain indication followed by gradual decrease over approx 330 seconds interval until measurement failure at ~EI+935		V12G9048A	
7.77	13:52:24	EI+495	X		Left Wing Front Spar at RCC Panel 9 - strain gage goes erratic for approximatly 20 second - measurement appears to be failing	Subsequent data is suspect	V12G9921A X1106.0 Y-229.0 ZMID	
7.8	13:52:25	EI+496	X		Left Outboard Elevon Wide Band Accelerometers - off-nominal vibration response (approximately 2G peak-to-peak) V08D9729A - L OB Elevon Z-Vib (MUX1B Ch 2)		V08D9729A	
7.85	13:52:29	EI+500	X		OMS-L Pod HRSI Surf T1-AFT - Start of slightly off-nominal erratic trend when compared to previous flights of same inclination	Followed by drop in temperature at EI + 570 seconds and subsequent erratic temperature changes	V07T9219A X1507.1 Y-126.0 Z422.0	
7.9	13:52:31	EI+502	X		Left Outboard Elevon Wide Band Accelerometers - off-nominal vibration response (approximately 3G peak-to-peak) V08D9729A - L OB Elevon Z-Vib (MUX1B Ch 2)		V08D9729A	
8	deleted					Rationale for deletion: moved to seq #8.7		
8.5	13:52:32/55	EI+503			Supply H2O Dump Nozzle Temps (A, B) (2) and Vacuum Vent Temp (1) - transient (15 and 23 seconds, respectively) increase in typical rise rates.	GMT shown indicates initial rise duration. Supply H2O Dump Nozzle temps took additional 48 secs to return to nominal temp rise, vacuum vent temps took additional 40 secs to return to nominal rise.	V62T0440A V62T0551A	V62T0439A
8.6	13:52:34	EI+505	X		OMS-L Pod HRS1 Surf T2-AFT - Start of off-nominal lower-than-expected temperature trend (compared to previous flights of same inclination) until sensor sees a sharp temp increase at EI+910 and goes erratic at EI+940		V07T9222A X1486.9 Y-126 Z422.0	
8.65	13:52:39 / 53:09	EI+510 / EI+540	X		4 Left OMS Pod Surface temps - Change in existing off-nominal temperature trend (following a cooler rise rate than expected, the temperature trend that is significantly warmer when compared to previous flights of same inclination)		V07T9976A V07T9220A	V07T9978A V07T9972A
8.7	13:52:41	EI+512			LMG Brake Line Temps (A, C) (2) - start of off nominal trend	Unusual Temperature Increase	V58T1700A	V58T1702A
8.75	13:52:44 / 52:50	EI+515 / EI+521			First clear indication of off-nominal aero increments	Delta yawing and rolling moment coefficients indicate off-nominal trends. Derived by analysis.	n/a	
8.8	13:52:49.5 / 52:51.4	EI+520.5 / EI+522.4	X		2 Left Wing temperature sensors begin an off-nominal (typically erratic) response that appears to be an indication of the measurements (sensors/wiring) failing		V09T9895A V09T9849A	
9	deleted							
10	13:52:59	EI+530			Left INBD Elevon Lower Skin Temp (1) - OSL	Began trending down 3 secs earlier	V09T1006A	
QBAR = ~25.5 psf (~0.18 psi); Mach 23.2					------ 32:13:53:00 ------		EI + 531 sec; WLE Stagnation Temp: ~2800 F	
10.5	deleted					Rationale for deletion: Merged with seq # 8.75 after further analysis.		
10.6	13:53:03	EI+534	X		Left Outboard Elevon Wide Band Accelerometers - onset of signal saturation indicating likely measurement failure (approximately 10G peak-to-peak - off-scale)		V08D9729A	
11	13:53:10 / 36	EI+541 / EI+567			Hydraulic System Left Outbd / Inbd Elevon Return Line Temps (4) - OSL	OSL was preceded by Nominal Temp rise.	V58T0394A V58T0157A	V58T0193A V58T0257A

STS-107 Mishap Investigation - Combined Summary Time Line
-BASELINE-

Integ Time Line Team - REV 17 BASELINE

5/8/2003 11 AM

Note: Rev 17 BASE integrates the OEX data timeline with the Baselined Rev 16 timeline plus IEE aero event changes (accounted for wind effects in aero increment derivation process).
Rev 17 was baselined by the OVE Working Group Team as of 5/7/03.

Sum No.	GMT GMT Day 32	EI sec	OEX data	Milestone	Entry Event	Remarks	MSID
11.1	deleted					Rationale for deletion: alpha modulation time tag updated - moved to seq #11.25	
11.2	13:53:26	EI+557		Approx Veh Grd Location: 38.7 N / -123.5 W	Altitude 231600 ft / Mach 23.0 - Crossing the California Coastline	Data source: STS-107 GPS Trajectory Data	
11.21	13:53:29	EI+560	X		Left Fuselage Side Surface Temp BP3605T - start of off-nominal increasing temperature trend from ~180 deg F to 400 deg F	Trend followed by temperature drop and rise	V07T9253A X1000.7 Y-105 Z354.5
11.22	13:53:29	EI+560	X		Left PLBD Surface TC BP3603T - Start of slightly off-nominal erratic temperature trend when compared to previous flights of same inclination		V07T9913A X1003.8 YLH Z441.3
11.23	13:53:29	EI+560	X		Left PLBD Surface TC BP3703T - start of off-nominal temperature rise, peaking at EI+625, followed by temperature drop and subsequent off-nominal higher-than-expected temperature signature		V07T9925A X1138.5 YLH Z441.4
11.24	13:53:29	EI+560	X		Left Fuselage Side Surface TC BP3604T - Start of slightly off-nominal erratic temperature trend when compared to previous flights of same inclination		V07T9903A X1006 Y-105 Z398.4
11.25	13:53:31	EI+562		Alpha Modulation	Angle of attack (alpha) modulation active		V90H0803C
11.3	13:53:32 / 54:22	EI+563 / EI+565			Two events of unexpected return link comm drop-out (Comm events 10-11)	On upper left aft antenna (TDRS 171/W). Appears off-nominal based on previous flt data. Comm loss not continuous thru period indicated.	
11.35	13:53:37	EI+568	X		Xo 1040 Spar (MLG Forward Wall Spar) Strain Gage - Upper Cap - start of off-nominal increase in strain indication (over an approximate 115 second interval) followed by sudden decrease		V12G9049A X1040 Y-135 ZUPR
11.37	13:53:38	EI+569			Inertial sideslip angle (Beta) exceeds flight history.	The steady state navigation derived sideslip angle becomes out-of-family as compared to previous flight data at this point in the trajectory.	V90H2249C
11.4	13:53:44	EI+575	X		OMS-L Pod HRSI Surf T1-AFT - Start of off-nominal lower-than-expected temperature trend when compared to previous flights of same inclination	Sensor goes erratic at EI+940	V07T9219A X1507.1 Y-126.0 Z422.0
11.5	13:53:45 / 54:11	EI+576 / EI+602			1st reported debris (5) observed leaving the Orbiter just aft of Orbiter envelope (Debris # 1 thru 5)	EOC video # EOC2-4-0055, 0056, 0064, 00136 & 0201. No evidence of jet firings near events.	n/a
QBAR = ~29 psf (~0.20 psi); Mach 22.7					------ 32:13:54:00 ------		EI + 591 sec; WLE Stagnation Temp: ~2850 F
12	deleted						
13	13:54:10 / 55:12	EI+601 / EI+663			Left Main Gear Brake Line Temp B (1) / Strut Actuator Temp (1) / Sys 3 LMG Brake Sw Vlv Ret Line Temp (FWD) (1) - start of off nominal trend	Unusual Temperature Increase	V58T1701A V58T0842A V58T0405A
14	13:54:20	EI+611			Start of slow aileron trim change; Reversal in trend of derived rolling moment coefficient.	The aileron trim setting observed in flight first deviates from the predicted trim setting at this pt in trajectory (GMT is approximate (+/- 10 sec) for aileron). Also, observed roll moment changed from a negative to positive slope (derived by analysis).	V90H1500C (aileron trim) n/a (roll moment)
15	13:54:22	EI+613			Mid Fuselage LT BondLine Temp at x1215 (1) & LH Aft Fus Sidewall Temp at x1410 (1) - start of off nominal trend	Unusual increase in temperature rise rate	V34T1106A V09T1724A
15.2	13:54:29	EI+620	X		Left Fuselage Side Surface temp BP3605T peaks and starts downward trend		V07T9253A X1000.7 Y-105 Z354.5
15.3	13:54:33.3 / 54:37	EI+624.3 / EI+628			Flash #1 - Orbiter envelope suddenly brightened (duration 0.3 sec), leaving noticeably luminescent signature in plasma trail; plus Debris # 6 - report of very bright debris observed leaving the Orbiter just aft of the Orbiter envelope.	EOC video # EOC2-4-0026, 0034, & 0009B. R3R and R2R jet firings occurred near events. Debris events 6 & 14 are visually the biggest, brightest events & therefore may indicate the most significant changes to the Orbiter of the western debris events.	n/a
15.32	13:54:34	EI+625	X		Left Fuselage Side Surface temp BP3703T peaks and starts downward trend		V07T9925A X1138.5 YLH Z441.5
13.33	13:54:39	~EI+630	X		Strain Gages Centered on the Upper Surface of the Left MLG Wheel Wheel - Higher-than-expected strain indications observed in these gages	Note: PCM3 entry data is in snapshot format (not continuous), therefore event may have occurred earlier than noted	V12G9156A, V12G9157A, V12G9158A

STS-107 Mishap Investigation - Combined Summary Time Line
-BASELINE-

Integ Time Line Team - REV 17 BASELINE

5/8/2003 11 AM

Note: Rev 17 BASE integrates the OEX data timeline with the Baselined Rev 16 timeline plus IEE aero event changes (accounted for wind effects in aero increment derivation process).
Rev 17 was baselined by the OVE Working Group Team as of 5/7/03.

Sum No.	GMT GMT Day 32	EI sec	OEX data	Milestone	Entry Event	Remarks	MSID
13.34	13:54:39	~EI+630	X		Left Wing X1040 Spar Web - shows increase in strain	Note: Adjacent sensor V12G9165A did not show similar "off-nominal" signature at this time, also, PCM3 entry data is in snapshot format (not continuous), therefore event may have occurred earlier than noted	V12G9166A V12G9167A (V12G9165A-nominal)
QBAR = ~34.5 psf (~0.24 psi); Mach 22.1					------ 32:13:55:00 ------		EI + 651 sec; WLE Stagnation Temp: ~2900 F
15.35	13:55:04 / 55:29	EI+655 / EI+680			Debris # 7, 7A, & 8 thru 10 observed leaving the Orbiter just aft of Orbiter envelope. Debris 8, 9, & 10 were seen aft of the Orbiter envelope inside Debris Shower A (next event listed).	EOC video # EOC2-4-0005, 0017, 0021, 0028, 0030, 0098 & 0161. No evidence of jet firings near events except 7A where analysis still pending.	n/a
15.37	13:55:22 / 55:28	EI+673 / EI+679			Debris Shower A - Report of debris shower seen just aft of Orbiter envelope.	Seen just aft of Orbiter envelope. Over the course of these four seconds a luminsecent section of plasma trail is observed which appears to contain a shower of indefinite particles and multiple, larger discrete debris that includes Debris 8, 9, and 10.	Saw debris: EOC2-4-0098, 0161, 0005, 0030 Saw shower: EOC2-4-0017, 0021, 0028
15.4	deleted					Rationale for deletion: Upon further evaluation of the data, it was determined that the remote sensor signatures had been seen in previous flights and/or could be explained by known events.	
15.43	13:55:33 / 56:03	EI+684 / EI+714			Two events of return link comm drop-outs (Comm events 12 & 13)	On upper right aft antenna (TDRS 171/W). Uncertain if off-nominal based on previous flight data. Comm loss not continuous thru period indicated.	
15.44	13:55:34	EI+685	X		Xo 1040 Spar (MLG Forward Wall Spar) Strain Gage - Upper Cap - sudden drop in strain followed by gradual increase until erratic signature at approximately EI+930		V12G9049A X1040 Y-135 ZUPR
15.45	13:55:35 / 56:13	EI+686 / EI+724			Debris # 11, 11A, 11B, 11C & 12 thru 15 observed leaving the Orbiter just aft of Orbiter envelope. Debris #11B & #11C events were both seen at the head of a parallel plasma trail aft of the Orbiter envelope. Debris #12 event was preceded and followed by secondary plasma trails. Debris #13 event was followed by momentary brightening of plasma trail adjacent to debris. Debris #14 event consisted of very bright debris observed leaving the Orbiter.	EOC video # EOC2-4-0005, 0017, 0021, 0028, 0030, 0050, & 0098. No evidence of jet firings near events. (Nearest jet firings occur at 56:17.) Debris events 6 & 14 are visually the biggest, brightest events & therefore may indicate the most significant changes to the Orbiter of the western debris events.	n/a
15.5	13:55:41	EI+692			Mid Fuselage Port (Left) Sill Longeron Temp at X1215 - start of off nominal trend	Unusual Temperature Increase	V34T1118A
QBAR = ~40 psf (~0.28 psi); Mach 21.4					------ 32:13:56:00 ------		EI + 711 sec; WLE Stagnation Temp: ~2900 F
16	13:56:03 / 56:24	EI+714 / EI+735			Left Lower/Upper Wing Skin Temps - Trending down (2)	Indication of potential measurement failures	V09T1002A V09T1024A
16.5	13:56:16 / 56:53	EI+727 / EI+764			Hyd Sys 1 LMG Uplock Actuator Unlock Line Temp; Sys 3 LMG Brake Sw Vlv Ret Line Temp (FWD); LMG Brake Line Temp C; LMG Brake Line Temp B; Sys 3 Left Main Gear Strut Actuator Temp - all show a temp rise rate change.	Significant increase in temp rise rate on all four lines	V58T0125A V58T1701A V58T0842A V58T0405A V58T1702A
16.55	13:56:30 / 56:55	EI+741 / EI+766			First Roll Reversal initiation / completion		V90H1044C
16.6	deleted					Rationale for deletion: Comm dropout (event 14) is deleted since probably nominal due to completion of roll reversal resulting in elevation angle nearing 60 deg's (vertical tail interfence w/comm).	
QBAR = ~42 psf (~0.29 psi); Mach 20.7					------ 32:13:57:00 ------		EI + 771 sec; WLE Stagnation Temp: ~2900 F
16.65	13:57:09	EI+780	X		Fuselage Side Surf Thermocpl BP3976T - start of off-nominal trend (temp increase followed by temp drop / rise)		V07T9270A X1486.1 Y-124.8 Z307.1
16.67	13:57:09	EI+780	X		Fuselage Lower Surface BF Thermocpl BP220T - start of off-nominal trend (shallow temp drop)		V07T9508A X1560 Y-111.1 Z LWR
16.7	13:57:19 / 24	EI+790 / EI+795			MLG LH Outbd Tire Pressures 1 & 2 - start of small increase in pressures	Not seen in previous flights	V51P0570A V51P0572A

STS-107 Mishap Investigation - Combined Summary Time Line
-BASELINE-

Integ Time Line Team - REV 17 BASELINE **5/8/2003 11 AM**

Note: Rev 17 BASE integrates the OEX data timeline with the Baselined Rev 16 timeline plus IEE aero event changes (accounted for wind effects in aero increment derivation process).
Rev 17 was baselined by the OVE Working Group Team as of 5/7/03.

Sum No.	GMT GMT Day 32	EI sec	OEX data	Milestone	Entry Event	Remarks	MSID	
16.8	13:57:19 / 58:01.5	EI+790 / EI+832.5			Debris # 16 (very faint debris) observed leaving just aft of Orbiter followed by two events of assymmetrcial brightening of the Orbiter shape (Flares 1 and 2). (Occurred over eastern AZ and NM.)	Debris #16: EOC video # EOC2-4-00148-2. Flares #1 & 2: EOC2-4-00148-4. Observations by personnel from the Starfire Optical Range (Kirtland Air Force Base, NM).	n/a	
17	13:57:28 / 57:43	EI+799 / EI+814			Left Lower/Upper Wing Skin Temps (2) - OSL		V09T1002A	V09T1024A
18	deleted							
19	13:57:54				Sys 2 LH Brake Sw Vlv Return Temp (1)	Unusual Temperature Increase	V58T0841A	
QBAR = ~52.5 psf (~0.36 psi); Mach 19.8					------ 32:13:58:00 ------		EI + 831 sec; WLE Stagnation Temp: ~2880 F	
20	13:58:03				Start of sharp aileron trim Increase	GMT is approximate (+/- 10 sec)	V90H1500C	
20.3	13:58:04	EI+835	X		Left fuselage side surface temp BP3605T starts off-nominal temperature increase		V07T9253A X1000.7 Y-105 Z354.5	
20.5	13:58:04 / 58:19	EI+835 / EI+850			Increase in off-nominal aero increments.	Substantial increase in rate of change of rolling and yawing moment increments and initial indication of off-nominal pitching moment increment. Derived by analysis.	n/a	
21	deleted							
22	deleted							
22.5	13:58:16	EI+847			LMG Brake Line Temp D - Temp rise rate change	Significant increase in temp rise rate.	V58T1703A	
23	13:58:32 / 58:54	EI+863 / EI+885			MLG LH Inbd / Outbd Tire Pressures (4) - Decay to OSL		V51P0570A V51P0571A	V51P0573A V51P0572A
24	deleted							
25	13:58:39 / 58:48	EI+870 / EI+879			MLG LH Inbd/Outbd Wheel Temps (2) - OSL		V51T0574A	V51T0575A
25.5	13:58:40	EI+871			BFS Fault Msg (4) - Tire Pressures - 1st Message			
26	13:58:56	EI+887			BFS Fault Msg (4) - Tire Pressures - Last Message			
QBAR = ~63.5 psf (~0.44 psi); Mach 18.7					------ 32:13:59:00 ------		EI + 891 sec; WLE Stagnation Temp: ~2850 F	
27	13:59:06				Left Main Gear Downlocked Indication - Transferred ON		V51X0125E	
27.3	13:59:09 / 59:39	EI+900 / EI+930	X		Several left side temperature measurements show a rapid increase in temperature followed by erratic behavior and subsequent loss of the measurements at approximately EI+940		V07T9925A V07T9972A V07T9976A V07T9903A V07T9913A	V07T9976A V07T9978A V07T9222A V07T9223A
27.5	13:59:23	EI+914			Loss of MCC real-time data to the workstations in the FCR and MER			
27.7	13:59:26 / 59:28	EI+917 / EI+919			Abrupt increase in off-nominal aero increments.	Abrupt increase in rate of change of pitching, rolling, and yawing increments. Magnitude of aero increments starting to exceed ability of aileron to laterally trim the vehicle. Derived by analysis.	n/a	
28	13:59:30.66 / 59:30.68	EI+921.66 / EI+921.68			Start of two yaw jets firing (R2R and R3R)	Fired continuously until end of data at 13:59:37.4	V79X2634X	V79X2638X
29	13:59:31	EI+922			Observed elevons deflection at LOS	Left: -8.11 deg (up) Right: -1.15 deg (up)		
29.3	13:59:31.4 / 59:34.5	EI+922.4 / EI+925.5			Several events and PASS and BFS FSM messages during this time period all indicate the failure signature of ASA 4	ASAs responded appropriately. However, signature is indicative of failure of ASA 4.	V57H0253A (5 Hz)	
29.5	13:59:32	EI+923			Observed aileron trim at LOS	-2.3 degrees		
30	deleted							
31	deleted							
32	deleted							
32.5	13:59:32	EI+923		Approx Veh Grd Location: 32.9 N / -99.0 W	Altitude ~200700 ft / Mach ~18.1 - Near Dallas TX	Approximate Vehicle Ground Location at Loss of Signal based on GMT; Data source: STS-107 GPS Trajectory Data	n/a	
33	13:59:32.136	EI+923.136		LOS	Last valid downlink frame accepted by ODRC - OI / BFS / PASS. Start of reconstructed data.	Nominal loss of comm at this GMT (for ~15 sec max based on previous flt data)		
34	deleted							
35	13:59:35/36	EI+926 / EI+927			Sideslip on vehicle changes sign.	The event occurred between the two times listed. Aerodynamic forces due to sideslip are now reinforcing aerodynamic asymmetry.	n/a	
36	13:59:36	EI+927			Growth in Bank attitude error	Up until this time the flight control had been able to maintain the Bank error around 5 deg.		
37	13:59:36.8	EI+927.8			Aerojet DAP Requests Third Right Yaw RCS Jet (R4R)	This additional jet is required to counteract the increasing aerodynamic moments on the vehicle. Fired continuously until end of data at 13:59:37.4		
38	13:59:37.3	EI+928.3			Aerojet DAP Requests Third Right Yaw RCS Jet (R1R)	This additional jet is required to counteract the increasing aerodynamic moments on the vehicle. Fired continuously until end of data at 13:59:37.4		

STS-107 Mishap Investigation - Combined Summary Time Line
-BASELINE-

Integ Time Line Team - REV 17 BASELINE

5/8/2003 11 AM

Note: Rev 17 BASE integrates the OEX data timeline with the Baselined Rev 16 timeline plus IEE aero event changes (accounted for wind effects in aero increment derivation process).
Rev 17 was baselined by the OVE Working Group Team as of 5/7/03.

Sum No.	GMT GMT Day 32	El sec	OEX data	Milestone	Entry Event	Remarks	MSID
39	13:59:37.n	EI+928.n			Last aileron data	The aileron position is now approx -5.2 deg with approx -2.5 deg of aileron trim. The rate of change of aileron trim had reached the maximum allowed by the flight control system.	
40	13:59:37.396	EI+928.396		End of 5-second period of reconstructed data	End of first 5-seconds of the 32-second period of post-LOS data. Start of approximately 25 seconds of no data available	GMT derived by MER data personnel	n/a
40.5	13:59:39 / 14:00:19	EI+930 / EI+970	X		Beginning at EI+930 and continuing until the loss of sync on OEX data (EI+964.4 for PCM and EI+970.4 for FDM), essentially all of the OEX data for the entire vehicle becomes erratic and fails		
41	13:59:46.347 / 14:00:01.900*	EI+937.347 / EI+952.900			PASS Fault Message annunciation - ROLL REF PASS Fault Message annunciation - L RCS LEAK BFS Fault Message annunciations - L RCS LEAK (2)	*Time info corrupted on some of the events.	
QBAR = nn psf; Mach nn					------ 32:14:00:00 ------		EI + 951 sec; WLE Stagnation Temp: ~2800 F
42	14:00:02/06	EI+953 / EI+957			Debris A observed leaving the Orbiter - Large debris seen falling away from the Orbiter envelope.	EOC videos # EOC2-4-0024, EOC2-4-0018 & EOC2-4-0118	n/a
43	14:00:02.654	EI+953.654			PASS Fault Message annunciation - L RCS LJET		
44	14:00:02.660	EI+953.660		Beginning of 2-second period of reconstructed data	Start of last 2-seconds of the 32 second period of post-LOS data.		
					During this final 2 second period of reconstructed data, the data indicates the following systems were nominal: APUs were running and WSB cooling was evident. MPS integrity was still evident. Fuel cells were generating power and the PRSD tanks/lines were intact. Comm and navaids systems in the forward fuselage were performing nominally. RSB, Body Flap, main engine, and right wing temps appeared active. ECLSS performance was nominal. During this final 2 second period of reconstructed data, the data indicates the following systems were off-nominal: All three Hyd systems were lost. The left inbd/outbd elevon actuator temps were either OSL or no data exists. Majority of left OMS pod sensors were either OSH or OSL or no data exists. Elevated temps at bottom bondline centerline skin forward and aft of the wheel wells and at the port side structure over left wing were observed. EPDC shows general upward shift in Main Bus amps and downward shift in Main Bus volts. AC3 phase A inverter appeared disconnected from the AC Bus. GNC data suggests vehicle was in an uncommanded attitude and was exhibiting uncontrolled rates. Yaw rate was at the sensor maximum of 20 deg/sec. The flight control mode was in AUTO. (Note that all Nav-derived parameters (e.g., alpha) are suspect due to high rates corrupting the IMU state.)		
45	14:00:03.470 / 14:00:03.637*	EI+954.470 / EI+954.637			BFS Fault Message annunciation - L OMS TK P BFS Fault Message annunciation - Indeterminant BFS Fault Message annunciation - SM1 AC VOLTS PASS Fault Message annunciation - L RCS PVT	* Time info corrupted on some of the events.	
46	14:00:03.637	EI+954.637			PASS Fault Message annunciation - DAP DOWNMODE RHC	The s/w process which logs the PASS message runs every 1.92 seconds, so this event could have occurred as early as 14:00:01.717 GMT. However, during the 2 sec period, available vehicle data indicates RHC was in detent and DAP was in AUTO.	
47	14:00:04.826	EI+955.826		End of 2-second period of reconstructed data	Last identifiable OI Downlink frame		n/a
47.5	14:00:13.439	EI+964.439	X		OEX PCM loss of sync		
48	14:00:17 / 14:00:22	EI+968 / EI+973			Debris B and C observed leaving the Orbiter	EOC videos # EOC2-4-0024 & -0118 (for both B and C)	n/a
48.5	14:00:19.44	EI+970.44	X		FDM1 A end of data		
49	14:00:21 / 14:00:25	EI+972 / EI+976			Vehicle Main Body break-up	EOC videos # EOC2-4-0024, -0018 &-0118	n/a
50	14:00:53	EI+1004		End of Peak Heating		Determined by analysis	

= Nominal/Expected Event or Performance